Journal of Hydrology: Regional Studies 59 (2025) 102337

Contents lists available at ScienceDirect

Journal of Hydrology: Regional Studies

journal homepage: www.elsevier.com/locate/ejrh

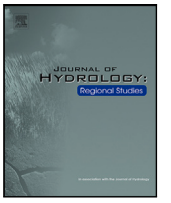

Three-stage hybrid modeling for real-time streamflow prediction in data-scarce regions

Awad M. Ali [a,b,1,*], Mohammed Abdallah [c,d,1], Babak Mohammadi [e], Hussam Eldin Elzain [f]

[a] Hydrology and Environmental Hydraulics Group, Wageningen University & Research, P.O. BOX 47, 6700AA, Wageningen, The Netherlands
[b] Water Research Center, Faculty of Engineering, University of Khartoum, P.O. BOX 321, Khartoum, Sudan
[c] College of Hydrology and Water Resources, Hohai University, Nanjing, Jiangsu 210024, China
[d] The Hydraulics Research Station, PO Box 318, Wad Medani, Sudan
[e] Hydrology Research Unit, Swedish Meteorological and Hydrological Institute, Norrköping, Sweden
[f] Water Research Center, Sultan Qaboos University, P.O. 50, AlKhoud 123, Muscat, Oman

ARTICLE INFO

Keywords:
PERSIANN family products
Conceptual hydrological modeling
Variational mode decomposition
Machine learning
Upper Blue Nile Basin

ABSTRACT

Study Region: The Upper Blue Nile Basin, Ethiopia
Study focus: This study addresses the challenge of utilizing satellite-based precipitation data in rainfall-runoff models for regions with limited ground observations. We propose a three-stage methodology incorporating Variational Mode Decomposition (VMD) into a conceptual data-driven framework (CHM-VMD-ML). The method was tested on four PERSIANN family precipitation products (2005–2019) using two conceptual hydrological models (CHM: HBV and GR6J) and three machine learning models (ML: Random Forest Regression, Boosted Regression Forest, and CatBoost Regression), with VMD applied to improve model inputs.

New hydrological insights: Our results highlight that integrating VMD significantly enhances the reliability of hydrological simulations driven by satellite precipitation data, particularly during low-flow periods. This approach reduces biases in PERSIANN products and improves overall model performance, as evidenced by an increase in Nash–Sutcliffe Efficiency values from 0.22–0.87 in the initial stage (CHM) to 0.74–0.92 in the final stage (CHM-VMD-ML). These findings underscore the importance of signal decomposition for refining data-driven models, facilitating better hydrological prediction and decision-making in data-scarce regions.

1. Introduction

Hydrological modeling plays a crucial role in understanding and managing water resources in various regions. The hydrological modeling of ungauged basins poses a significant challenge in the field of hydrology (Khan et al., 2010). An ungauged basin lacks the valuable data that is essential for traditional hydrological models. Therefore, the reliance on remote sensing data becomes an essential alternative to fill this data gap and enhance the hydrological modeling performance. Satellite-based meteorological data play the role of functional and alternative datasets, providing spatial and temporal variation over large areas (Lauri et al., 2014; Xu

* Corresponding author at: Hydrology and Environmental Hydraulics Group, Wageningen University & Research, P.O. BOX 47, 6700AA, Wageningen, The Netherlands.
E-mail addresses: awad.negmeldinawad.mohammedali@wur.nl (A.M. Ali), m.abdallah.hhu@gmail.com (M. Abdallah), babak.mohammadi@smhi.se (B. Mohammadi), halzain944@gmail.com (H.E. Elzain).
[1] These authors contributed equally to this work and should be considered co-first authors.

https://doi.org/10.1016/j.ejrh.2025.102337
Received 4 July 2024; Accepted 19 March 2025
Available online 5 April 2025

et al., 2014). Due to the advantages of remote sensing datasets, previous studies have proved successful implementation of remote sensing information on ungauged basins (Maswood and Hossain, 2016; Poortinga et al., 2017; Andriambeloson et al., 2020; Nguyen et al., 2023).

One widely used satellite precipitation product is the PERSIANN (Precipitation Estimation from Remotely Sensed Information using Artificial Neural Networks) family product (Hsu et al., 1997), which employs infrared data sourced from geostationary satellites for the purpose of rainfall estimation through the utilization of artificial neural networks. It converts gridded infrared data from satellites like GOES-8, GOES-10, GMSfall-5, Metsat −6, and Metsat −7 into precipitation rates with 0.25° ×0.25° resolution for various time steps (1, 3, 6 h, and daily) (Kunnath-Poovakka and Eldho, 2023). PERSIANN family products offer some advantages to overcome the limitations of precipitation measurement in ungauged catchments and large areas. The PERSIANN family includes various versions, such as PERSIANN, PERSIANN-CCS, PERSIANN-CDR, and PERCIANN-CCS-CDR. The PERSIANN family products (such as PERSIANN-CCS) can provide near-real-time precipitation estimates across large, remote, or inaccessible areas, making them particularly useful for ungauged basins (Nguyen et al., 2018; Sadeghi et al., 2021; Salehi et al., 2022). Moreover, PERSIANN systems provide continuous, high-resolution spatial (0.25° ×0.25° and 0.04° ×0.04°) and temporal (hourly and daily) rainfall data, which is essential for accurate and dynamic hydrological modeling. Periodic enhancements to the precision of the PERSIANN-CCS system are achieved through consistent updates that incorporate microwave-derived rainfall estimates obtained from low-orbit satellites (Sorooshian et al., 2000). This globally available dataset has been widely used in hydrological modeling studies to improve the representation of precipitation inputs and enhance the performance of models in ungauged basins (Khoshchehreh et al., 2020; Le et al., 2020; Salehi et al., 2022). However, some studies showed poor performance of the PERSIANN family products in hydrological modeling across the Blue Nile basin (Bitew and Gebremichael, 2011). Bias-correction in the context of remote sensing-based precipitation products, such as those from the PERSIANN family, is crucial for enhancing the accuracy and reliability of precipitation data, therefore it is recommended to implement a bias-correction approach (Xiao et al., 2022) for the PERSIANN family products within the daily time intervals and this issue can be considered as a limitation for the application of PERSIANN family products (Eini et al., 2022). These techniques are vital for adjusting remote sensing data so that they more closely match observed ground truth data. However, the effectiveness of bias correction methodologies is heavily dependent on the availability and density of ground-based gauge stations.

The water resources of the Nile River depend heavily on the Upper Blue Nile Basin (UBNB) in Ethiopia, making it crucial to acknowledge the UBNB's role in Nile River water management (Asmamaw, 2015; Digna et al., 2017). However, the basin faces various challenges, including the construction of the Grand Ethiopian Renaissance Dam (GERD) (Nasr and Neef, 2016), climate change impacts (Mengistu et al., 2021), and downstream water management issues (Ali et al., 2023). Moreover, the UBNB is the source of most of the Nile's flow, on which millions of people in downstream countries (i.e., Sudan and Egypt) depend for their livelihoods. To address these challenges effectively, accurate hydrological modeling is essential in this basin, which facilitates a comprehensive understanding of the hydrological and climatic factors affecting the basin. However, a significant challenge lies in the accessibility of extended hydro-climatic data within the basin over an extended duration (Dile et al., 2018). A considerable portion of the basin lacks gauge instrumentation, and the existing gauges lack continuous monitoring and maintenance, leading to questionable data reliability (Jain Figueroa, 2012; Hussien, 2014; Allam, 2017). Additionally, uneven distribution of existing gauges and errors due to instrument defects further complicate the examination of the basin's natural processes. Improving hydrological modeling input via satellite-based data is crucial in river basins like the UBNB, where there is a scarcity of data and limited or poor-quality hydrological and meteorological measurements. In order to achieve improved accuracy in hydrological modeling for the UBNB, the integration of reliable data sources and advanced data-driven tools with a conceptual hydrological model can increase the model capability.

A machine learning (ML) model has the ability to recognize patterns within data and generate predictions or decisions without knowledge about the phenomenon (Lary et al., 2016; Kumar et al., 2019). These models have demonstrated efficacy through their successful application across diverse fields, including hydrological studies, where they are used to make accurate hydrological predictions (e.g., streamflow) (Li et al., 2022; Kumar et al., 2023) and improve the performance of conceptual hydrological models (Okkan et al., 2021; Roy et al., 2023; Mohammadi et al., 2024). In the realm of hydrological modeling, ML stands out for its capability to handle complex and non-linear relationships between variables (Mosaffa et al., 2022). This sets it apart from traditional methods which often struggle in this regard. Moreover, ML has the advantage of being able to handle large and diverse datasets, making it a valuable tool for integrating various types of information such as remote sensing data into hydrological models (Lange and Sippel, 2020). On the other hand, the relatively recent introduction of the variational mode decomposition (VMD) technique has gained recognition for its adaptive signal decomposition algorithm and its effectiveness has been demonstrated in several areas, including hydrology (Seo et al., 2018; Sibtain et al., 2021; Abdallah et al., 2023; Ahmadi et al., 2023). VMD can break down a signal into a set of sub-signals with adjustable and adaptable bandwidths (Dragomiretskiy and Zosso, 2013; Chen et al., 2019), which can identify and extract important features and patterns in the original data and leads VMD to find more information from hydrological and meteorological time series data. The combination of ML and VMD techniques offers several advantages in hydrological modeling and this type of integration can improve the model's ability to capture the complex dynamics and non-linear relationships within the hydrological system, leading to more accurate hydrological simulation.

Both ML and VMD have shown great potential for improving the accuracy and reliability of hydrological modeling in various climates (He et al., 2019; Zuo et al., 2020). For instance, Dibike and Solomatine (2001) utilized ML techniques such as artificial neural networks (ANNs) to model rainfall-runoff processes and found them to outperform traditional modeling methods in terms of prediction accuracy. Similarly, Govindaraju (2000) reviewed the application of data-driven methods in hydrology and concluded that ML approaches could handle non-linearity and complexity better than traditional methods. Regarding VMD, Rehman and Mandic

(2010) introduced the concept and demonstrated its effectiveness in decomposing complex signals into intrinsic mode functions with limited and adaptive bandwidths. In the context of hydrology, VMD has been used by Hu et al. (2021) to decompose daily streamflow data into several sub-signals, which were then modeled separately to improve prediction accuracy.

The integration of ML and VMD has also been explored in some studies. For example, He et al. (2019) used signal decomposition techniques (such as VMD) to decompose runoff data into multiple sub-signals, and then the deep learning model was applied as a predictor model to forecast daily runoff, resulting in the best performance for VMD simulated based runoff compared to the empirical mode decomposition (EMD) and ensemble EMD approaches. For instance, in a study by Seo et al. (2018), VMD was applied to partition input and target time series into constituent sub-time series. The study developed machine learning models, including Extreme Learning Machine (ELM) and Least Squares Support Vector Machines (LSSVR), coupled with VMD to model daily rainfall-runoff processes. The results showed that the VMD-ELM and VMD-LSSVR models outperformed the ELM and LSSVR models without VMD. In another study by Wu et al. (2023a), an ensemble deep-learning model was formulated for the prediction of runoff across three hydrological stations. In their study, they employed explainable artificial intelligence alongside meteorological variables harnessed from ensemble models within the realm of deep learning to facilitate the accurate runoff prediction. The results showed that the model outperformed traditional models in terms of accuracy and interpretability. In a recent investigation conducted by Zhang et al. (2023), an innovative coupled model, VMD-SSA-BiLSTM, was introduced for the prediction of monthly runoff in the lower Yellow River. The application of VMD in signal processing effectively reduced the noise inherent in the original runoff series, extracting intricate and pertinent information embedded in the runoff data. Subsequently, the Singular Spectrum Analysis (SSA) technique was employed to refine the BiLSTM model, optimizing key parameters such as the number of hidden units, maximum training period, and initial learning rate. This optimization significantly enhanced the efficiency of model parameter selection. The integrated VMD-SSA-BiLSTM model demonstrated notable accuracy in predicting runoff, as evidenced by high levels of accuracy during the training and testing phases.

In this study, we propose a three-stage framework (CHM-VMD-ML) to explore integrating ML and VMD techniques for reducing uncertainty in satellite-based precipitation products in simulating discharge within conceptual hydrological models (CHMs). We use PERSIANN family products as a case study to model discharge in the UBNB. Then, the specific objectives of this study can be introduced as: (1) to evaluate the effectiveness of two CHMs (namely HBV and GR6J) in simulating daily discharge using different satellite-based precipitation products (SPPs) over the period from 2005 to 2019; (2) to explore the potential of three ML models namely Random Forest Regression (RFR), Boosted Regression Forests (BRF), and Catboost Regression (CBR) in conjunction with the outputs of the conceptual hydrological models and meteorological variables; and (3) to assess the impact of coupling VMD techniques with CHM-ML models on improving the accuracy and reliability of discharge simulations, particularly among the different seasons.

2. Study area and data

2.1. Study area

The UBNB in Ethiopia is situated in the eastern segment of the Nile basin, as depicted in Fig. 1a, and holds significance as a major contributor to the Nile River, encompassing an area of approximately 176,000 km^2. The topography within the basin exhibits a descent from high altitudes in the north-east, reaching up to 4261 m.a.s.l at Ras Dashen Mountain, to the lowest elevation of 489 m.a.s.l at the western outlet, as illustrated in Fig. 1b. Notably, an average annual flow of about 50 km^3 of water occurs through the Ethiopia-Sudan border, specifically at the Eldiem station, with pronounced seasonality, as 80% of this flow takes place solely from July to October (Kim and Kaluarachchi, 2009). Moreover, the UBNB experiences varying annual rainfall ranging from 200 mm in the north-east to 2200 mm in the south-west Fig. 1c. Additionally, the annual potential evapotranspiration ranges from 1000 to 1800 mm (Conway, 2000), while air temperature in the region fluctuates between 13 and 26 °C (Tekleab et al., 2013).

Our particular focus on the UBNB stems from the challenges posed by the construction of the Grand Ethiopian Renaissance Dam (GERD) and the ongoing political tensions involving Ethiopia, Sudan, and Egypt (Turhan, 2021). These circumstances have resulted in a lack of transparency, and difficulties in data sharing and underscore the necessity for an enhanced modeling framework to effectively manage downstream areas, as highlighted by Ali et al. (2023).

2.2. Hydrometeorological datasets

2.2.1. Ground observations

The absence of readily available and accessible ground observations poses a challenge and serves as a driving force for our research. Fourteen ground stations of precipitation during the period 2006–2019 were obtained from the National Meteorological Agency (NMA) of Ethiopia. The stations are unevenly distributed and mostly located in the center of the basin as shown in Fig. 1b. A brief summary of rainfall stations' location and elevation is illustrated in Table S.1 in the supplemetary materials.

The daily discharge measurements for the Eldiem hydrometric station were collected from the Ministry of Irrigation and Water Resources of Sudan (MoIWR) from 2006 to 2019. It is noteworthy that the discharge measurement at the Eldiem station is derived through the utilization of rating curves established on observed water levels. Commencing from 2012, the Eldiem Station has encountered the influence of the backwater effect stemming from the Roseires dam, particularly in the filling months spanning from June to October. Within this time frame, the MoIWR computes the outflow from the Roseires dam via water balance assessments (Ali et al., 2023). Data from January 1, 2005, to December 31, 2015, were used in this work to calibrate our two CHMs and train the coupled ML models. Following that, the models' performance was verified using data ranging from January 1, 2016, to December 31, 2019. For the CHMs, a warm-up phase was also considered using data of the first year (i.e., 2015). The time series graph of daily discharge is illustrated in Fig. 2.

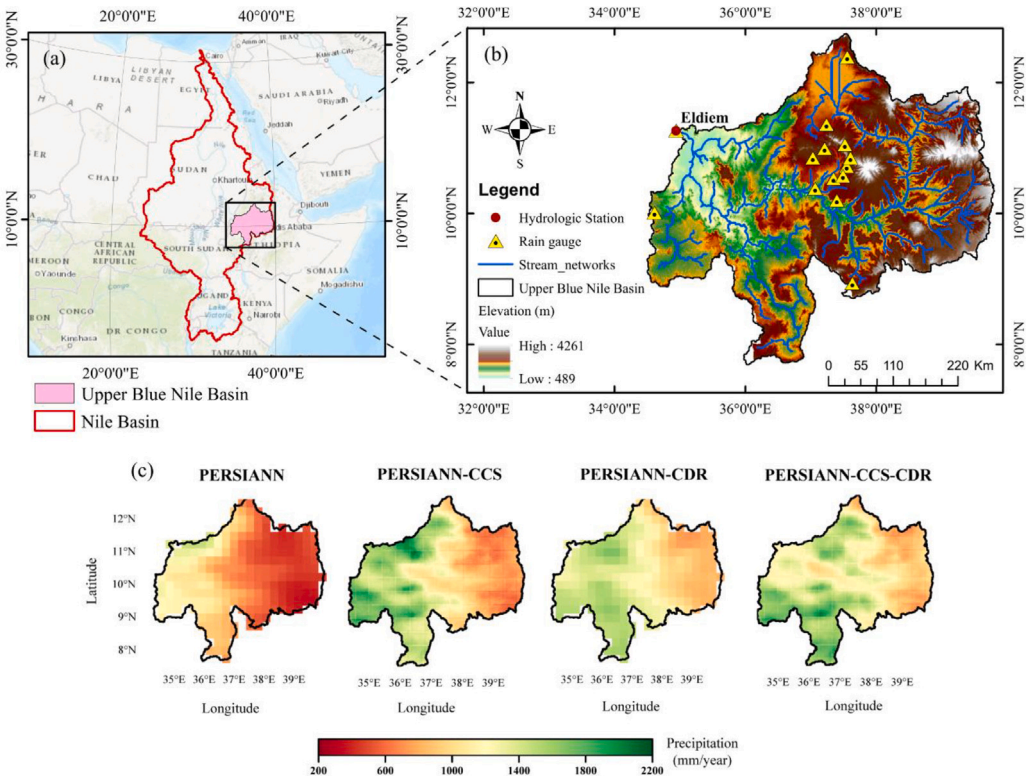

Fig. 1. Hydrometeorological data pertaining to the UBNB. (a) Geographical location of the UBNB within the Nile basin. (b) Visualization of the river network, and discharge and rain gauging stations. (c) Annual precipitation averages for the period (2005–2019), were computed using PERSIANN, PERSIANN-CCS, PERSIANN-CDR, and PERSIANN-CCS-CDR datasets.

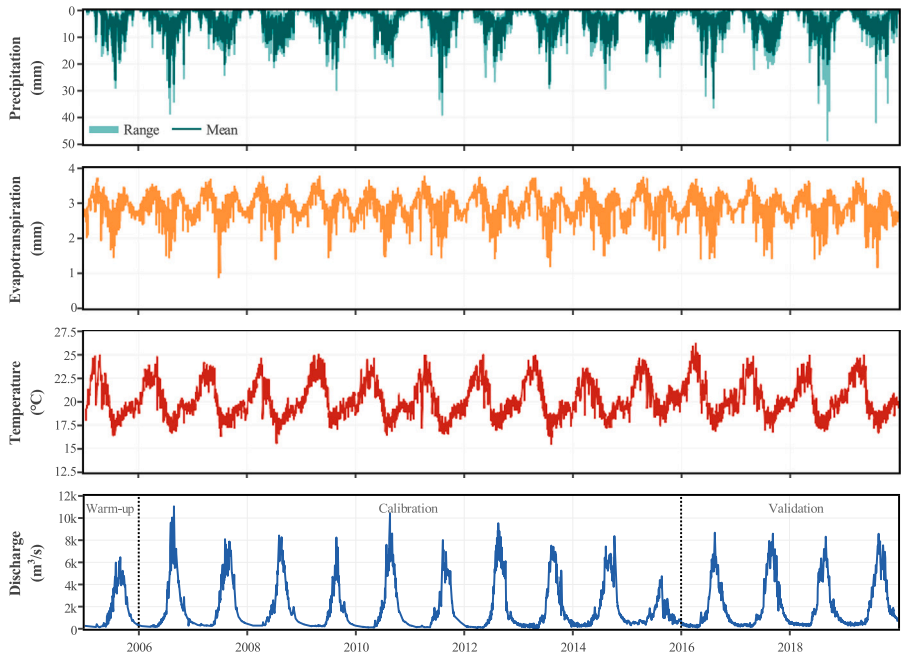

Fig. 2. Time series graph of input datasets to conceptual hydrological models and observed discharge during the full modeling period (2005–2019). We display precipitation from the PERSIANN family products range (light green line) and mean (green line), mean potential evapotranspiration from GLEAM v3.7a (orange line), mean temperature from ERA5 (red line), and discharge at Eldiem station from MoIWR (blue line). (For interpretation of the references to colour in this figure legend, the reader is referred to the web version of this article.)

Table 1
Information of selected remote sensing datasets to force two conceptual hydrological models over the UBNB from 2005 to 2019.

Input	Products	Spatial resolution	Temporal resolution	Time span	Bias Correction
Precipitation	PERSIANN	0.25° × 0.25°	hourly to yearly	2000–present	No
	PERSIANN-CCS	0.04° × 0.04°	hourly to yearly	2003–present	No
	PERSIANN-CDR	0.25° × 0.25°	daily to yearly	1983–present	Yes
	PERSIANN-CCS-CDR	0.04° × 0.04°	3-hourly to yearly	1983–present	Yes
Temperature	ERA5	0.25° × 0.25°	Hourly	1950–present	–
Potential Evapotranspiration	GLEAM 3.7a	0.25° × 0.25°	daily to yearly	1983-present	–

2.2.2. Satellite-based precipitation products

Four products of satellite-based precipitation from the PERSIANN family were used for the analysis in this study which are PERSIANN, PERSIANN-CCS, PERSIANN-CDR, and PERSIANN-CCS-CDR were collected from the Center for Hydrometeorology and Remote Sensing (CHRS) Data Portal. The characteristics of the products are provided in Tabel 2. The time series graph during the study period (range and mean value) from PERSIANN family products is illustrated in Fig. 2.

PERSIANN is a real-time across the world with high-resolution satellite precipitation products (Hsu et al., 1997). The rainfall rate is estimated by the present operational PERSIANN using neural network functionality (classification/approximation) algorithms. Its main input was originally longwave infrared images from geostationary orbiting (GEO) satellites, but it was subsequently expanded to incorporate visible imagery taken during the day. During the availability of independent rainfall estimations, its adaptive training function changes the network parameters.

PERSIANN-Cloud Classification System (PERSIANN-CCS) is a global product with a high spatial resolution (Hong et al., 2004). It categorizes cloud patch properties by taking into account satellite-retrieved information regarding cloud height, areal breadth, and texture variation. These categories assist in determining the quantity of precipitation that should be attributed to each cloud's pixel according to a specific curve depicting the relationship between precipitation rates and brightness temperature.

PERSIANN-Climate Data Record (PERSIANN-CDR) has given a near-global precipitation dataset since January 1983 (Ashouri et al., 2015). It was created to meet the demand for an ongoing and consistent global precipitation dataset that would help in various climate-related investigations. It is an altered form of the PERSIANN approach that uses GEO satellite infrared images as the primary data source for the ANN model. Nevertheless, unlike the PERSIANN approach, which uses passive microwave imaging for updating the network's configuration parameters, PERSIANN-CDR develops the ANN model utilizing Stage IV hourly precipitation obtained from the National Centers for Environmental Prediction (NCEP). The approach is subsequently employed to estimate historical information using predefined parameters. The estimations are then bias-corrected for the whole-time frame in record utilizing the Global Precipitation Climatology Project (GPCP) dataset. However, there is approximately a three-month delay in the public availability of the dataset (Nguyen et al., 2018).

PERSIANN-CCS-CDR is intended to alleviate earlier products' shortcomings by delivering precipitation amounts with high spatiotemporal precision and over a longer time of record (Sadeghi et al., 2021). PERSIANN-CCS-CDR integrates the techniques used in the development of PERSIANN-CCS and PERSIANN-CDR and uses information from GEO satellites as inputs in order to generate highly accurate spatiotemporal precipitation datasets with an extended record span. The PERSIANN-CCS method is used to globally merge infrared output from the Gridded satellite (GridSat-B1) and NOAA Climate Prediction Centre (CPC-4 km) in this procedure.

2.2.3. Temperature and potential evapotranspiration

For hydrological modeling, daily mean air temperature information above 2 meters from 2005 to 2019 was collected from ERA5. Model-based 4D-Var data assimilation approach was used by the European Centre for Medium-Range Weather Forecasts (ECMWF) to produce the global datasets (Hersbach et al., 2019).

In this study, the daily average potential evapotranspiration (PET) time series was obtained from the Global Land Evaporation Amsterdam Model (GLEAM) version 3.7a during the study period. The GLEAM PET information was derived from various reanalysis datasets using the Priestley-Taylor algorithm based on surface radiation and near-surface air temperature (Miralles et al., 2011). Recently, several studies employed GLEAM products in the field of hydrometeorology applications since developed (Jiang et al., 2021; McNamara et al., 2021; Wang et al., 2022; Alghafli et al., 2023). The average daily time series is illustrated in Fig. 2 while a description of PET GLEAM product was provided in Table 1.

3. Methodology

The procedural framework employed in our investigation, aimed at accomplishing the aforementioned objectives, is briefly illustrated in Fig. 3. The initial phase involved both continuous and categorical statistical assessment to evaluate the performance of various PERSIANN family products in comparison to the depicted rain stations in Fig. 1b. Following this, an exploration into improving the reliability of conceptual hydrological modeling was conducted through a comparative analysis of simulated discharge outcomes across three distinct stages.

In the first stage, we forced two CHMs namely GR6J and HBV, utilizing daily temperature, potential evapotranspiration, and four PERSIANN precipitation products as described in Section 2.2.2. Moving to the second stage, the diverse outputs from each CHM, integrated with satellite-based meteorological products, served as inputs for three tree-based ML models; RFR, BRF, and CBR. The

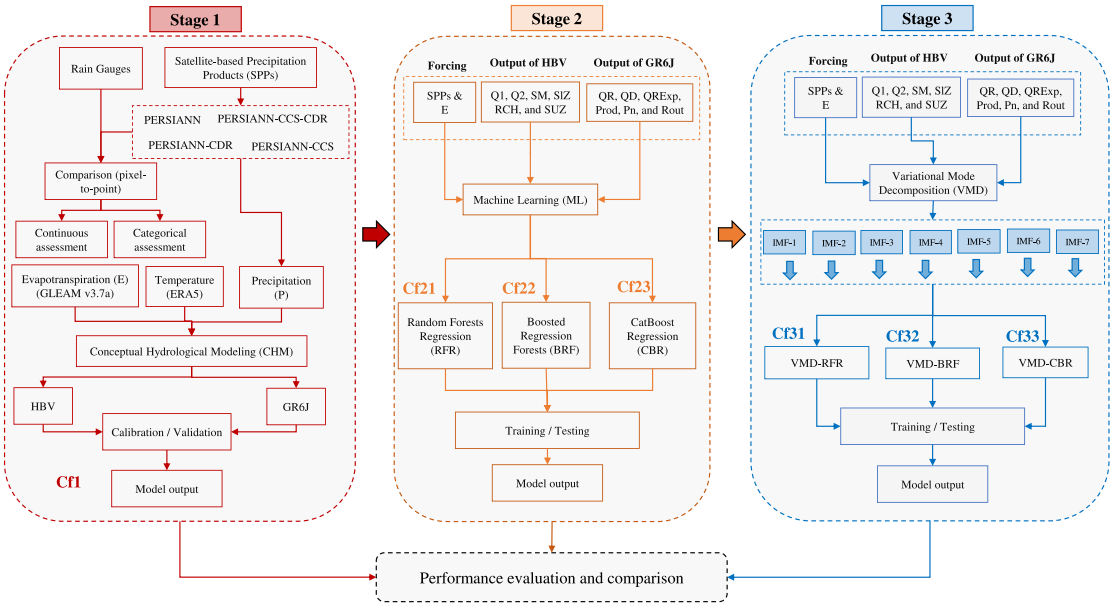

Fig. 3. Flow chart illustrating the implemented rainfall-runoff modeling framework. Our approach initiates with the assessment of satellite-based precipitation products, followed by three modeling stages: CHM, CHM-ML, and CHM-VMD-ML. Our work concludes with a comparative analysis of the simulated discharge across the three stages.

final stage replicated the preceding one, with the differentiation being the utilization of inputs to drive the ML models after signal decomposition using VMD techniques. For clarity in the result description and discussion, we delineate distinct model configurations denoted by 'Cf' followed by a two-part numeric code indicating the stage number (1: CHM, 2: CHM-ML, 3: CHM-VMD-ML) and ML model number (1: RFR, 2: BRF, 3: CBR). It is pertinent to note that in the initial stage where ML models are not employed, only one configuration exists, denoted as Cf1. In the following subsections, we offer a detailed and comprehensive explanation of the methodology we have employed.

3.1. Conceptual hydrological modeling (CHM)

3.1.1. GR6J model

The GR6J is introduced by Pushpalatha et al. (2011) as conceptual hydrological model can be utilized for rainfall-runoff modeling, with six parameters (X_1 to X_6) related to the production store, routing and exponential routing stores, unit hydrograph, and groundwater exchange (Poncelet et al., 2017; Crochemore et al., 2020). In order to determine the optimal parameter values, the GR6J model uses meteorological input data, including air temperature, potential evaporation, and precipitation while a discharge as a reference. The GR6J model initially calculates net precipitation (P_n) and actual evapotranspiration (AET), then the production storage level ($Prod$), routing store level ($Rout$), routing store outflow (Q_R), exponential store outflow (Q_{REXP}), and direct flow (Q_D). Finally, the simulated flow is computed by adding Q_R, Q_{REXP}, and Q_D together. The GR6J model can be calibrated manually or automatically using Michel's approach (Michel, 1987) while there are four objection criterion functions called Nash–Sutcliffe Efficiency (NSE; Nash and Sutcliffe (1970)), Kling–Gupta efficiency (KGE; Gupta et al. (2009)), modified KGE (KGE′; Kling et al. (2012)), and RMSE. In this study, we employed the lumped model structure of GR6J, with the automatic Michel calibration techniques and NSE as objective function. The parameter ranges for calibrating the model are shown in Table 2. In this regard, a preliminary screening procedure is performed for parameter sets or predetermined grids. Then, by starting with the process of screening findings the steepest descent local search method is satisfied. In this study, daily streamflow was simulated using PERSIANN family products across the UBNB.

3.1.2. HBV-light model

The Hydrologiska Byråns Vattenavdelning (HBV) represents a conceptual rainfall-runoff model devised by Bergström (1995). This model is applicable in both lumped and semi-distributed forms, proficiently simulating discharge in large catchments with minimal input data and parameters. In our investigation, we employed the HBV-light, a lumped variant recognized for its efficiency in capturing hydrological nuances in the UBNB, as highlighted by Ali et al. (2023). HBV-light incorporates daily averaged precipitation, temperature, and potential evapotranspiration to model daily discharge, following the four main routines: snow, soil moisture, groundwater and response, and routing. Based on model inputs and parameters, the model calculates the water content in the soil box (SM) and the recharge to the groundwater (RCH), then estimates the storage in the upper (SUZ) and lower (SLZ)

Table 2
Parameter setting of the HBV and GR6J model with a description of each parameter and optimal value for each product.

Model	Parameter	Description	Range	PERSIANN	PERSIANN -CCS	PERSIANN -CDR	PERSIANN -CCS-CDR
HBV	FC	Maximum soil moisture (mm)	[200, 1000]	340.69	1000	1000	1000
	LP	Soil moisture threshold for evaporation reduction	[0.5, 0.7]	0.62	0.50	0.50	0.50
	BETA	Shape coefficient	[1, 4]	1.38	2.02	2.12	2.19
	PERC	Maximum flow from upper to lower groundwater box (mm d^{-1})	[1.4, 2.8]	1.40	1.40	1.40	1.40
	UZL	Threshold for K0 outflow (mm)	[10.2, 25.6]	25.60	25.60	25.60	25.60
	K0	Recession coefficient (d^{-1})	[0.05, 0.2]	0.05	0.05	0.05	0.05
	K1	Recession coefficient (d^{-1})	[0.01, 0.2]	0.076	0.13	0.11	0.10
	K2	Recession coefficient (d^{-1})	[0.006, 0.05]	0.05	0.05	0.05	0.05
	MAXBAS	Length of weighting function (day)	[1.5, 2.9]	2.90	1.70	2.90	1.81
GR6J	X1	Capacity of the production store (mm)	[0, 200]	0.00	0.00	0.00	21.46
	X2	Groundwater exchange coefficient (mm)	[−5, 6]	−1.17	−1.22	−3.96	−5.33
	X3	Capacity of the non-linear routing store (mm)	[0, 1000]	421.03	300.68	491.88	499.23
	X4	Unit hydrograph time base (day)	[0.5, 20]	4.33	4.20	4.14	3.81
	X5	Catchment exchange threshold	[−2.0, 2.0]	0.25	−0.05	0.21	0.24
	X6	Exponential store depletion coefficient	[0, 200]	17.32	165.67	31.97	34.99

groundwater boxes. The final discharge is simulated as the sum of the three runoff components; rapid surface flow (Q_0), slow surface flow (Q_1), and base flow (Q_2) taking the routing into account. Optimization of the model is achieved through Monte Carlo or GAP optimization methods within predefined parameter ranges. In our research, we utilized GAP optimization with NSE as the objective function, guided by parameter ranges specified in Table 2 based on Ali et al. (2023). Given the absence of snow in the study area, our discharge simulations exhibit insensitivity to the snow routine parameters. Similar to the GR6J model, HBV-light was forced using the four precipitation products from the PERSIANN family, along with ERA5 and GLEAM 3.7a.

3.2. Machine learning models

In this section, a theoretical description of several advanced models will be provided, including RFR, BRF, and CBR models as well as the VMD techniques to enhance predictive accuracy of rainfall-runoff modeling. These models play a crucial role in advancing hydrological research and improving the accuracy of hydrological predictions, thereby contributing to better water resource management and decision-making (Zounemat-Kermani et al., 2021).

3.2.1. Random Forest Regression (RFR)

The RFR is an adaptable and robust ensemble learning algorithm introduced by Breiman (2001). The concept of RFR is based on decision trees to create a powerful predictive regression model. Instead of relying on a single decision tree, it builds multiple trees independently, each trained on a random subset of the training data and a random subset of features. The training of RFR uses a technique called bagging to create diverse sets of training data for each tree. It randomly selects samples with replacements from the original training dataset to create multiple bootstrap samples. The bootstrap sample is employed to partition and shuffle the dataset into uniformly distributed subsets. Each tree is trained using randomly selected subsets from this bootstrapped dataset. Typically, two-thirds of the dataset is utilized within the bootstrap sample, while the remaining one-third is left out. These left-out samples, referred to as out-of-bag (OOB) samples, are used for estimating the out-of-bag error (OOBE). The OOB-error rate is utilized to validate the performance accuracy of the model. Once all the trees are trained, predictions are made by averaging the predictions of all individual trees in the forest.

In hydrology, RFR is often utilized for its ability to handle nonlinear relationships between hydrological variables. It excels in capturing complex interactions and non-linearities in hydrological data, making it suitable for tasks such as evapotranspiration modeling (Douna et al., 2021), flood prediction (Tan et al., 2024), groundwater vulnerability (Giri et al., 2023), and water quality estimation (Harrison et al., 2021; Elzain et al., 2024).

3.2.2. Boosted Regression Forest (BRF)

BRF is a machine learning ensemble technique introduced by Friedman (2001) which that combines the concepts of both boosting and random forests to create a powerful predictive model. In BRF, boosting is applied to a collection of decision trees, where each new tree is trained with a specific form of boosting to minimize the loss function with respect to the predictions of the existing ensemble. However, each tree is trained on a random subset of the training data and a random subset of features, similar to random forests. This hybrid approach leverages the strengths of both boosting and random forests to create a robust and accurate predictive model. BRF aggregates the predictions from all the trees in the ensemble to make predictions for new data points. The final prediction is the sum of the predictions of individual trees, weighted by their respective contributions to the model.

BRF is valuable in hydrology for its capability to sequentially refine models and improve predictive performance. It is particularly useful for capturing subtle relationships and patterns in hydrological data, thereby enhancing the accuracy of predictions in tasks such as streamflow forecasting (Katipoğlu and Sarı göl, 2023) and drought monitoring (Bueechi et al., 2023).

3.2.3. CatBoost Regression (CBR)

CBR is a powerful algorithm and presents a permutation-based alternative to traditional algorithms and represents an innovative approach for handling categorical features within the modeling process (Prokhorenkova et al., 2018). It combines the flexibility of gradient boosting with the efficient handling of categorical data, making it a popular choice for a wide range of regression problems. CBR is built upon the gradient-boosting framework. Gradient boosting is an ensemble learning technique where a series of weak learners, typically decision trees, are built sequentially to correct the errors of the preceding models. The final prediction is the sum of the predictions of all the individual trees. CBR incorporates various regularization techniques to prevent overfitting. These include controlling the depth of the trees, using a leaf-wise tree growth strategy, and considering combinations of features. CBR combines predictions from all the trees in the ensemble to make predictions for new data points. CBR has gained popularity in hydrology for its efficient handling of categorical variables and robustness to noisy data (Huang et al., 2019; Wang et al., 2023b; Elzain et al., 2024).

3.2.4. Variational mode decomposition (VMD)

VMD is a signal processing technique introduced by Dragomiretskiy and Zosso (2013). It is designed for the decomposition of a given signal into a set of oscillatory components called intrinsic mode functions (IMFs). This method is particularly effective for analyzing non-stationary and multi-component signals. VMD operates on the assumption that a signal can be expressed as the sum of a finite number of modes with varying frequencies. The theory of VMD involves an optimization problem that tries to find these IMFs by minimizing a cost function.

$$min_{u_k}\{\Sigma_{k=1}^{K}(\frac{1}{2}\|x-u_k\|_2^2+\gamma\varphi(u_k))\} \quad (1)$$

$u_k(t)$ represents the kth mode, and the optimization is carried out over all i-k modes simultaneously. The first term $\frac{1}{2}\|x-u_k\|_2^2$ enforces fidelity to the original signal, ensuring that the modes accurately represent the input signal. The second term $\varphi(u_k)$ introduces a regularization parameter γ to control the smoothness of each mode. The regularization term $\gamma\varphi(u_k)$ penalizes the roughness or complexity of the mode, promoting simpler and more interpretable solutions. The optimization problem is typically solved using an iterative algorithm that alternates between updating the modes and the Lagrange multipliers. The resulting decomposition provides a set of modes that capture different oscillatory components present in the signal. The modes are sorted in order of increasing frequency, allowing for the identification and analysis of different spectral components. The mathematical foundation of VMD, rooted in optimization theory and regularization, enables effective signal decomposition and mode extraction, contributing to the understanding and interpretation of complex signals in diverse applications.

In our framework, the VMD approach was adopted to decompose the meteorological variables (SPP and E) and the output of the HBV (SM, RCH, SUZ, SLZ, Q_1, and Q_2) or GR6J (Q_D, Q_R, Q_{RExp}, P_n, Q_{Prod}, $Rout$) models into a sequence of IMFs with varying frequency (Fig. 3). The total number of decomposition levels is acknowledged to have a significant impact on model accuracy (Wen et al., 2019; Abdallah et al., 2023). This study employed VMD techniques with a parameter such as moderate bandwidth limit ($\alpha = 5000$), noise tolerance ($\tau = 0$), omega initialization ($init = 0$), convergence tolerance ($tol = 0.000001$), and decomposition layer ($K = 7$) based on prior studies (Ali et al., 2021; Kang et al., 2022).

VMD models are increasingly applied in hydrology for their ability to decompose complex hydrological time series data into distinct modes or components (Gan et al., 2021). This decomposition allows for a better understanding of underlying patterns and dynamics in hydrological processes, aiding in tasks such as streamflow prediction (Ahmadi et al., 2023) and drought forecasting (Ekmekcioğlu, 2023).

3.3. Performance evaluation

To conduct a comprehensive assessment and comparison of the simulated discharge resulting from the three stages, our evaluation employed a range of methodologies, including statistical metrics, flow-duration curves, and seasonal analysis.

Adhering to the evaluation guidelines outlined by Moriasi et al. (2007), we employed three statistical metrics; NSE, ratio of RMSE to measured standard deviation (RSR), and Percent bias (PBIAS) for a primary evaluation. Firstly, with a focus on the results of HBV and GR6J, we explored the performance of PERSIANN family products during both the calibration (2006–2015) and validation (2016–2019) periods. This allowed us to gain insights into the limitations associated with the use of each product in conventional modeling. Second, we compared the overall performance changes attributed to the introduction of ML models without

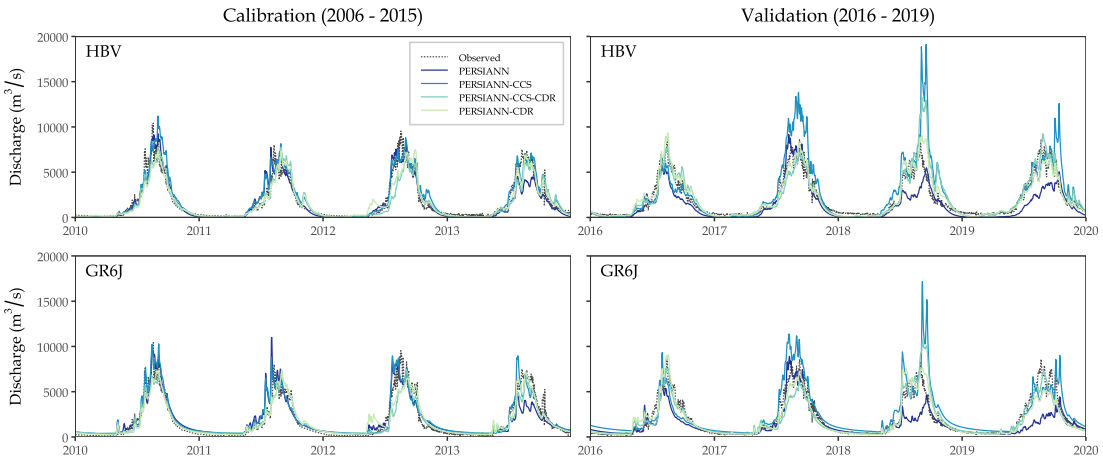

Fig. 4. Comparison of daily hydrograph of observed (dotted black line) and simulated discharge data using HBV (first row) and GR6J (second row) models forced by PERSIANN (dark blue line), PERSIANN-CCS (cyan line), PERSIANN-CCS-CDR (light teal line), and PERSIANN-CDR (ligh green line) during calibration (left column) and validation (right column) period. Note that, we show only a four-year time series span (2010–2013) for visibility of results in the calibration period. (For interpretation of the references to colour in this figure legend, the reader is referred to the web version of this article.)

(Stage 2) and with (Stage 3) VMD techniques. This comparative analysis provided an understanding of the implications introduced by the additional steps. Additionally, we employed the flow-duration curve to further comprehend the alterations in discharge brought about by the different stages. This also facilitated an understanding of the sensitivity of the approach to the selection of the hydrological model and the machine learning algorithm. Lastly, we delved into the impact of the different stages on the four seasons: MAM (March-May), JJA (June-August), SON (September-November), and DJF (December-February). This enabled us to highlight the significance of adding new stages for diverse hydrological applications. In this analysis, we also incorporated a Taylor diagram for a more thorough assessment (Taylor, 2001).

4. Results

4.1. Simulated discharge from stage 1 (CHM)

Fig. 4 shows the hydrograph of observed and simulated daily discharge, by forcing PERSIANN family products into HBV and GR6J models, during the calibration and validation periods. The optimized parameter values of both models are presented in Table 2. During the calibration phase, the hydrograph shows an acceptable performance in simulating the daily discharge of all PERSIANN family products according to HBV and GR6J models. However, PERSIANN, PERSIANN-CCS, and PERSIANN-CCS-CDR products indicate poor performance in capturing the peak flow during the validation period. On the contrary, the PERSIANN-CDR product well-capturing both low and peak flows.

We evaluated the simulated daily discharge against observed discharge using numerous statistical metrics, the finding of which are reported in Table 3. During the calibration phase, all PERSIANN family products simulate daily discharge with good performance through the two CHMs. While during the validation phase, the PERSIANN-CCS product simulates daily discharge with unsatisfactory performance when forced in the HBV model (NSE = 0.21, RSR = 0.89, and PBIAS = 28.51%). This high bias indicates the overall positive bias (i.e., overestimation) over the basin, which was also noticed in GR6J (PBIAS = 24.12%). On the contrary, the PERSIANN-CCS-CDR product indicates good performance and PERSIANN-CDR indicates very good performance during the validation phase. PERSIANN product resulted in the highest negative bias with PBIAS of −30.85 (HBV) and −27.69 (GR6J).

The distinct model structures of HBV and GR6J models resulted in different model performances when employing the same input datasets. However, both models agreed on the ranking of the products, with PERSIANN-CDR resulting the best performance, followed by PERSIANN-CCS-CDR, PERSIANN, and PERCIANN-CCS. These results are affected by the performance of the products in capturing the rainfall magnitudes during the validation years, thus suggesting the need for further approaches to improve their predictive skills.

4.2. Simulated discharge using the three-stage framework (CHM-VMD-ML)

The statistical performance of simulated daily discharge data during the validation period based on the three-stage approach is illustrated in a matrix for each statistical metric (Fig. 5) and Table 4. Cf1 corresponds to the outcomes detailed in Section 4.1, with NSE ranging from 0.21 to 0.87, RSR ranging from 0.39 to 0.89, and PBIAS ranging from −31% to 29%. Cf2 exhibits the results of CHM-ML which use meteorological data and output component of HBV and GR6J models with the three ML models including RFR

Table 3
Performance evaluation of simulated daily discharge using HBV and GR6J when forced by PERSIANN family products.

Model	Product	Calibration (2006–2015)			Validation (2016–2019)		
		NSE (-)	RSR (-)	PBIAS (%)	NSE (-)	RSR (-)	PBIAS (%)
HBV	PERSIANN	0.76	0.49	−6.82	0.67	0.58	−30.85
	PERSIANN-CCS	0.77	0.48	3.59	0.21	0.89	28.51
	PERSIANN-CCS-CDR	0.81	0.43	3.79	0.71	0.54	9.30
	PERSIANN-CDR	0.85	0.38	2.12	0.87	0.36	3.45
GR6J	PERSIANN	0.72	0.53	2.89	0.56	0.67	−27.69
	PERSIANN-CCS	0.81	0.44	3.39	0.55	0.67	24.12
	PERSIANN-CCS-CDR	0.86	0.38	2.53	0.80	0.45	−3.35
	PERSIANN-CDR	0.87	0.37	2.00	0.86	0.38	−4.78

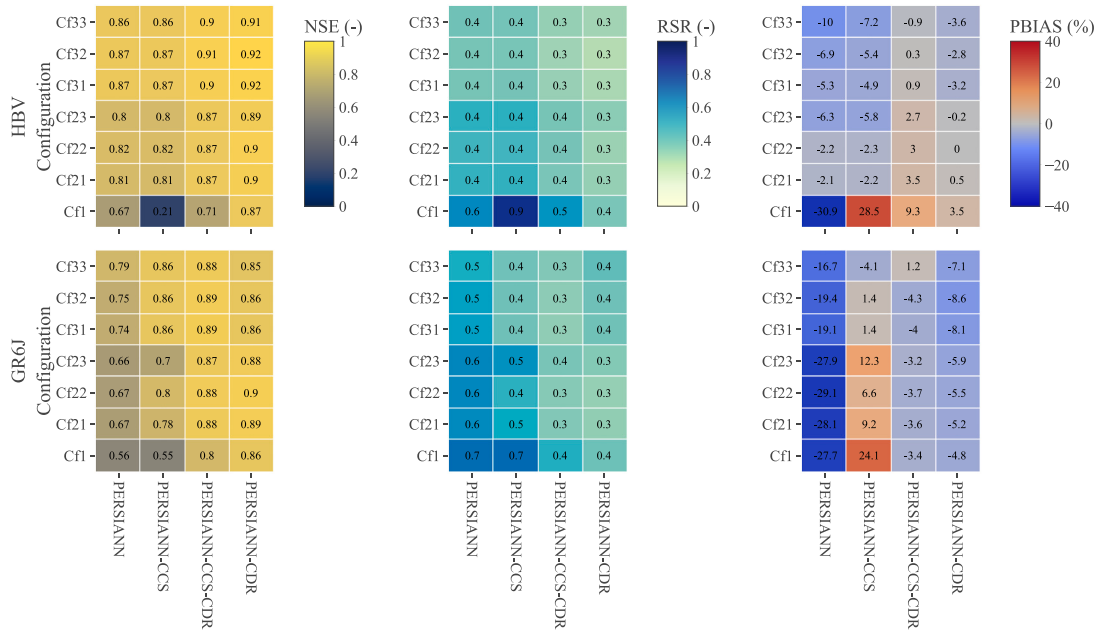

Fig. 5. Enhanced discharge predictions across stages. Cf1 corresponds to the standalone CHM, Cf2 denotes the CHM-ML configuration, and Cf3 signifies the CHM-VMD-ML configuration. The numerical designation following each configuration indicates the machine learning algorithm (1: RFR, 2: BRF, 3: CBR).

Table 4
Performance range of simulated daily discharge using HBV and GR6J at each stage during the validation period. The minimum and maximum values are based on the three ML and four PERSIANN family products.

Model	Configuration	NSE (-)		RSR (-)		PBIAS (%)	
		Min.	Max.	Min.	Max.	Min.	Max.
HBV	Cf1: CHM	0.21	0.87	0.36	0.89	−30.85	28.51
	Cf2: CHM-ML	0.80	0.90	0.31	0.45	−6.26	3.46
	Cf3: CHM-VMD-ML	0.86	0.92	0.27	0.37	−9.96	0.87
GR6J	Cf1: CHM	0.55	0.86	0.38	0.67	−27.69	24.12
	Cf2: CHM-ML	0.66	0.90	0.32	0.58	−29.15	12.3
	Cf3: CHM-VMD-ML	0.74	0.89	0.33	0.51	−19.45	1.42

(Cf21), BRF (Cf22), and CBR (Cf23). Cf2 is remarkably better than Cf1 for all statistical metrics, products, and model combinations (NSE of 0.66–0.90, RSR of 0.31–0.58, and PBIAS of −29%–12%). Furthermore, a noticeable improvement is evident in the third stage (Cf31, Cf32, and Cf33), representing the outcomes of CHM-VMD-ML. In comparison to the second stage, the application of VMD techniques increased the accuracy of simulated daily discharge and reduced uncertainty related to model input (i.e., PERSIANN family products) resulted in NSE of 0.74–0.92, RSR of 0.27–0.51, and PBIAS of −19%–1.4%. Nevertheless, in HBV results, the bias experienced a marginal rise following the incorporation of VMD, a phenomenon attributable to the trade-off between bias and variance affecting the overall performance.

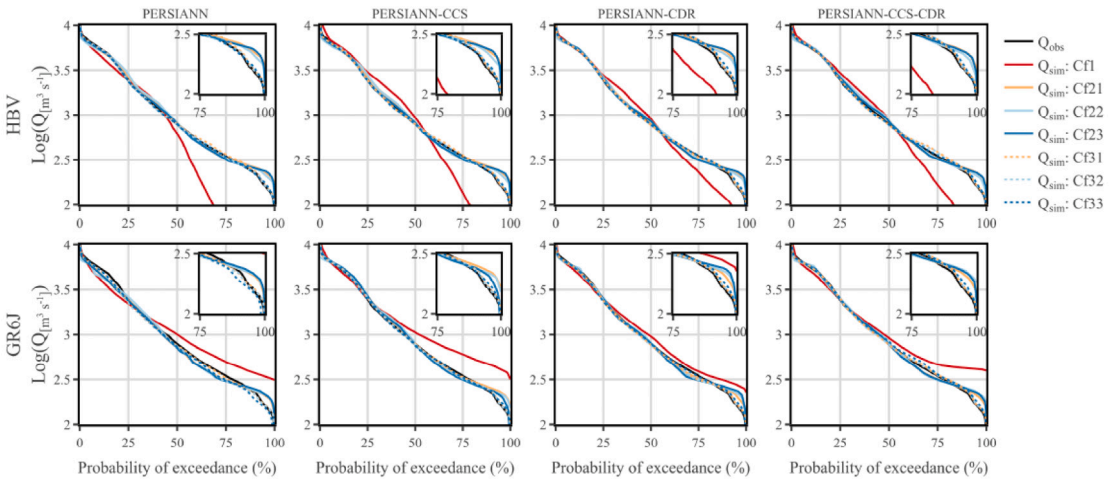

Fig. 6. Flow-duration curves comparing observed (black line) and simulated discharges at the UBNB outlet. The top row illustrates outcomes generated by the HBV model, while the bottom row displays results obtained from the GR6J model. The solid-colored lines represent outputs from Cf2, whereas the dotted lines represent outputs from Cf3. It is important to note that the smaller panels provide a zoomed-in view of the low-flows (probability of exceedance ≥ 75%) of each corresponding panel.

We analyzed the flow duration curve to delve deeper into the contributions of the three stages, as illustrated in Fig. 6. In the initial phase involving standalone models (i.e., Cf1), it became evident that HBV consistently underestimated flows with a probability of exceedance surpassing 50%, while GR6J notably overestimated such flows. Within the PERISANN family products, PERSIANN-CDR stands out by exhibiting the least disparities with the actual discharge curve in both CHMs. Transitioning to Cf2, we observed a significant enhancement in matching the flow curve across all levels of exceedance. In the third stage, the application of VMD techniques resulted in the most substantial improvement in simulating discharge, compared to Cf1 and Cf2, particularly in low-flow conditions (refer to the zoomed panels in Fig. 6). The discharge curves of Cf3 closely aligned with the actual discharge curve, emphasizing the significance of incorporating VMD for accurately representing extreme discharge events.

4.3. Seasonal (comparative) analysis

To gain deeper insights into the enhancements achieved through the incorporation of the VMD, we conducted an analysis using the Taylor diagram, focusing on the least effective precipitation product (i.e., PERSIANN-CCS) across the four seasons: MAM, JJA, SON, and DJF (Fig. 7). Assessing the performance of the two CHMs and three ML algorithms, we observed an incremental improvement as we progressed through successive stages, with notable advancements particularly evident from Cf1 to Cf2. Notably, our findings imply that the signal decomposition of ML predictors (i.e., Cf3) led to heightened correlation, reduced error, and diminished relative variability (manifested as a smaller disparity between simulated and observed standard deviation).

To assess performance variations across seasons, we examined the relative change in RMSE compared to Cf1 (Fig. 8). For the HBV simulated discharge, the most significant enhancements occurred in SON, with an average RMSE change of −66.4% for Cf2 and −73.4% for Cf3. In the case of GR6J, the maximum improvement was observed in the DJF, showing an average change of −70.7% for Cf2 and −78.4% for Cf3.

Furthermore, when comparing the last two stages, VMD-related improvement was consistently observed across different seasons, with the most substantial enhancements occurring at the onset of the high-flow season (JJA) with an averaged enhancement of −21.7% for HBV and −24.9% for GR6J. This was followed by enhancements in the low-flow season (MAM) with an averaged enhancement of −20.7% for HBV and −21.6% for GR6J. Notably, the introduction of VMD eliminated differences among ML algorithms, resulting in fewer discrepancies. These results indicate that, using the variational mode decomposition within a conceptual data-driven model has the potential to increase the reliability of satellite precipitation products.

5. Discussion

5.1. Hydrological modeling sensitivity to the quality of SPPs

Precipitation is a critical meteorological variable for understanding hydrological processes, managing water resources, and long-term climate research (Shayeghi et al., 2020; Gebremicael et al., 2022). Precipitation input errors can cause significant uncertainty in discharge simulations (Alfieri et al., 2014; Wang et al., 2021). Previous research indicates that the uncertainty of rainfall data accounts for between 70% and 80% of the error in discharge simulations (Gebregiorgis and Hossain, 2012). In the UBNB, precipitation was identified as the primary source of uncertainty in discharge estimation, accounting for 45% of the annual

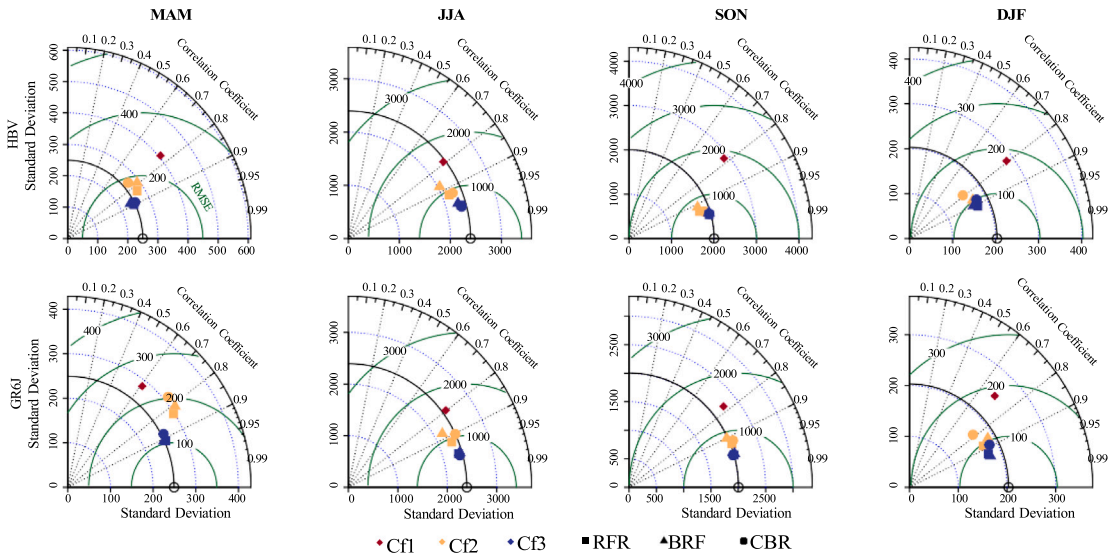

Fig. 7. Taylor diagram illustrating simulated discharges forced by PERSIANN-CCS (during validation period from 2016 to 2019) throughout the four distinct seasons (MAM, JJA, SON, and DJF). The top row showcases outcomes derived from the HBV model, while the bottom row presents results obtained from the GR6J model. Discrete stages are distinguished by color, with CHM represented in red, CHM-ML in yellow, and CHM-VMD-ML in blue. Various ML algorithms are denoted by distinct shapes, including RFR represented by squares, BRF by triangles, and CBR by circles.

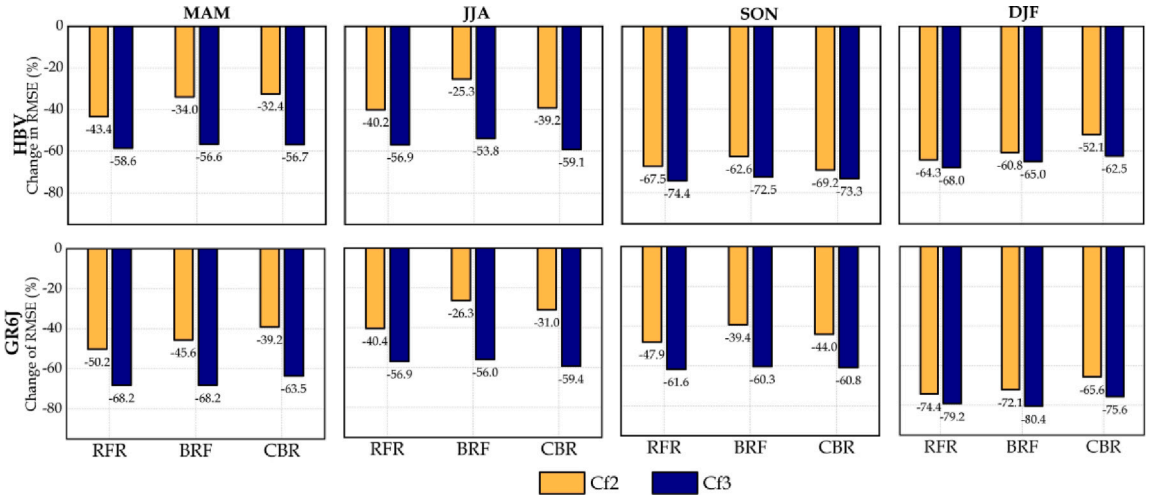

Fig. 8. Relative RMSE change for three ML algorithms across MAM, JJA, SON, and DJF, assessed at Cf2 and Cf3 with Cf1 as reference. Top row: outcomes from the HBV model. Bottom row: results from the GR6J model. These results were calculated for the simulated discharge forced by PERSIANN-CCS product during the validation period (2016–2019).

average uncertainty (Alghafli et al., 2023). Unfortunately, ground rainfall observations are inadequate or absent in many localities, particularly in poor countries (Behrangi et al., 2011). High-density precipitation observation networks are essential to capture the peak flow (Bárdossy and Anwar, 2023). In areas that are poorly, unevenly distributed, or ungauged, SPPs are increasingly becoming a necessary choice for getting reliable precipitation data (Alriah et al., 2022). The assessment of SPPs using observed streamflow data through the hydrological modeling enables the ongoing exploration of error propagation associated with these products, as opposed to direct comparison with gauge rainfall-based statistical metrics (Camici et al., 2018; Satgé et al., 2019; Nawaz et al., 2021).

The performance of PERSIANN family products in precipitation estimation and discharge simulation varied across different regions. For example, daily precipitation estimations and discharge simulations using PERSIANN family products are unsatisfactory (KGE with range −9.0 to 0.22) across the Wełna catchment in Poland (Eini et al., 2022). Also, Salehi et al. (2022) stated that the PERSIANN family products failed to capture the peak of simulated daily, monthly, and winter discharge during the period of 2012–2018 over the Russian River catchment in California. Some studies reported the poor performance of PERSIANN family

products in hydrological simulation across the Nile Basin (Bitew and Gebremichael, 2011; Bitew et al., 2012; Gebere et al., 2015; Gebremicael et al., 2022). However, the PERSIANN-CDR product indicates better performance and is comparable to other products over the Nile Basin (Guermazi et al., 2019; Musie et al., 2019; Gebremicael et al., 2022; Ali et al., 2023) and other regions (Zhu et al., 2016; Bâ et al., 2018; Ma et al., 2018).

It is noteworthy that the accuracy of simulated discharge is closely linked to the quality of input precipitation and other datasets. Within the realm of hydrological applications, the PERSIANN family provides a suite of products tailored to diverse needs. Notably, PERSIANN-CDR exhibits superior statistical and categorical performance when compared to alternative products (Figure S.1 and S.2 in the supplementary materials). This distinction is attributed to the incorporation of bias corrections derived from the GPCP precipitation dataset (Khan et al., 2010). As a result, hydrological models driven by PERSIANN-CDR demonstrate the most favorable discharge outcomes (Table 3 and Fig. 4). In light of this, the diminished performance of alternative products, particularly PERSIANN-CCS, hinders their reliability for intended purposes of real-time monitoring and hydrological forecasting. Therefore, relying solely on CHM, developing reliable flood early warning system is challenging due to the high biases introduced by PERSIANN and PERSIANN-CCS (Fig. 4).

5.2. CHM-VMD-ML framework opportunities

Recently, a great effort has been made to enhance precipitation estimation by merging multiple satellite products with ground observation stations based on statistical approaches. Their application in hydrological simulation resulted in reducing the uncertainty of individual products and improved the accuracy of discharge simulation (Ma et al., 2018; Ur Rahman et al., 2020). However, such merging approach needs a very high density of observation network to well represent the catchment, which is not available in many regions including the UBNB. Moreover, the recommended bias-correction of PERSIANN family (Xiao et al., 2022) is no longer feasible. Due to these constraints, we proposed to use the VMD techniques and ML models based on meteorological data and output of CHM to improve the reliability of PERSIANN family products to simulate daily discharge. This is particularly relevant for low-latency but biased products (i.e., PERSIANN and PERSIANN-CCS), enabling robust real-time discharge prediction. The use of decomposition with ML models proved to be beneficial to different hydrological studies such as estimating the reference evapotranspiration (Kang et al., 2022), solar radiation (Abdallah et al., 2023), discharge simulation (Sezen and Partal, 2022), vegetation periodic changes (Wang et al., 2023a).

In this study, we endeavored to enhance the effectiveness of conceptual hydrological models through the application of ML algorithms. A remarkable deficiency in the initial stage is the substantial disparity noted between observed and simulated below-average flows (i.e., exceeding a 50% probability of exceedance). These flows exhibit underestimation by the HBV model and overestimation by the GR6J model (Fig. 6). Besides the quality of the SPPs, this disparity can be attributed to the utilization of NSE as the objective function, a metric known for its insensitivity to low-flow conditions (Steinfeld et al., 2015). The integration of ML algorithms (in Cf2) significantly improved the performance of the conceptual models across all flow values, aligning with findings from prior research. Notably, the incorporation of Long Short-Term Memory (LSTM) neural networks in a hybrid model with HBV and GR6J resulted in enhanced performance compared to their standalone configurations (Xiong et al., 2021; Yu et al., 2023). Moreover, the implementation of the random forest algorithm reduced prediction uncertainty in the HBV-PF model, thereby enhancing overall predictive accuracy (Roy et al., 2023). Therefore, Cf2 outperformed Cf1 due to the ability of ML algorithms to capture non-stationarity, noise complexity, and non-linear relationships (Yaseen et al., 2015), thus better link CHM's outputs with observed discharge.

Moreover, we aimed to investigate the opportunities offered by introducing the VMD in the modeling framework. Given our analysis of the different stages, it is clear that the decomposition of the meteorological datasets and CHM outputs is most likely to outperform the performance of ML without the VMD. This improvement was found to be more noticeable from May to August as demonstrated in Fig. 8. Therefore, such an approach provides a promising opportunity and contributes towards more reliable modeling thus informed decision making in data-scarce regions. A previous study employed a hybrid model based on decomposed GR6J outputs using wavelet transformation and an artificial neural network (Sezen and Partal, 2022). The study concluded that the hybrid model outperformed the individual conceptual and data-driven models in three tested subbasins in Turkey. Another hydrogeological study compared five ML models with their hybrid wavelet models and attributed the improvement made by the wavelet-transform due to its capability to capture the non-linearity and seasonality of the data (Samani et al., 2023). In summary, implementing our proposed framework helps mitigate the shortcomings found in PERSIANN family products, thereby enhancing their reliability for their intended uses.

5.3. Limitations and future perspectives

In the course of our investigation, certain considerations were omitted, though with an expected marginal impact on the outcomes, yet not on the fundamental conclusion. First, the choice of the objective function is anticipated to influence the relative enhancements achieved in the subsequent stages. For instance, employing log (NSE) as an alternative metric would likely yield superior performance of the CHMs during low-flow periods, potentially compromising accuracy in capturing peak flows due to its insensitivity to high-flow events (Krause et al., 2005). In that case, the subsequent stages are projected to result in improvements during seasons characterized by high-flow regimes. Second, the construction of the Grand Ethiopian Renaissance Dam at the basin's outlet, coupled with the start of its filling operations in 2020, introduces alterations to downstream water availability (Ali et al., 2023). Despite this, we maintain confidence in the resilience of our fundamental conclusion. Notably, methodologies such as

random forest have demonstrated suitability for quantifying human activities and climate change impacts on alterations in discharge patterns (Liu et al., 2022). Third, our reliance was exclusively on tree-based algorithms; however, the incorporation of VMD markedly enhanced the performance of models utilizing deep learning approaches, such as LSTM and Convolutional Neural Networks (Wu et al., 2023b).

We acknowledge several limitations that are important to consider for a comprehensive understanding of the current research. The current study heavily depends on the quality and availability of SPPs, and any gaps or inaccuracies in these data sets could significantly impact the outcomes of the modeling results. Additionally, our evaluation of PERSIANN family products was based on gauging stations that are clustered in the center of the UBNB (see the supplementary materials). Therefore, our evaluation is not representative for the whole basin. In analogous situations, we suggest utilizing other comprehensive evaluation approaches such as the Triple collocation method (Stoffelen, 1998) or its extended version (McColl et al., 2014). In another view, this research focuses on the UBNB, which raises questions about the generalizability and transferability of our findings to other geographic locations or hydrological contexts. Different regions with unique hydrological characteristics might require adjustments to the model or different approaches altogether. Also, integrating VMD with CHM and ML models introduces a level of complexity that could pose challenges in computational resources, model calibration, and interpretation of results, particularly if integrated into distributed hydrological models. The intricate nature of this situation requires a delicate equilibrium between the sophistication of the model and its practical applicability. In addition, the study's emphasis on daily discharge simulations implies that our results may not be directly applicable to alternative temporal scales, such as hourly or monthly runoff forecasts. Hydrological processes may demonstrate diverse behaviors at different temporal scales, thus requiring distinct modeling methodologies. Additionally, the complex task of quantifying the uncertainties that naturally arise in the modeling process, particularly when incorporating various advanced techniques, persists. The uncertainties associated with these factors play a crucial role in shaping the decision-making processes within water resource management. Consequently, accurately quantifying these uncertainties is of utmost importance to effectively apply our research findings.

A potential field for future investigation involves the implementation and evaluation of our proposed modeling framework in various hydrological settings beyond the UBNB. This would aid in evaluating the model's capacity to generalize and adapt to diverse climatic conditions, topographies, and land-use patterns. To improve the handling of intricate nonlinear relationships within hydrological processes, future studies may examine the application of advanced algorithms, such as deep learning and neural networks. There is also a need for more robust methods to quantify uncertainties in both the input data and the model outputs. This might involve incorporating event-based modeling techniques and analyzing extreme value statistics. Understanding the impacts of climate change on the performance of the proposed modeling framework is an important research aspect. This involves the analysis of how shifts in precipitation patterns, temperature, and other climatic variables could potentially influence the reliability and accuracy of the proposed framework.

6. Conclusion

In summary, our study introduces a three-stage data-driven framework integrating machine learning and variational mode decomposition techniques to address the challenges associated with satellite-based precipitation products in the UBNB. The primary goal is to reduce uncertainty and enhance the accuracy of (real-time) discharge simulations, thereby advancing conceptual hydrological models. By simulating discharge through the integration of decomposed signals from a calibrated conceptual hydrological model outputs and meteorological satellite data into a machine learning algorithm, our framework demonstrates consistent improvements across various stages. During the validation period (2016–2019), the NSE values ranged from 0.22 to 0.87 in stage 1, improved to a range of 0.66 to 0.90 in stage 2, and further enhanced to a range of 0.74 to 0.92 in stage 3. Importantly, the observed improvements are not only statistically significant but also hold consistent across different seasons, reinforcing the framework's efficacy in capturing diverse hydrological conditions. For example, during the high-flow season onset (JJA), coupling the less reliable SPP (i.e., PERSIANN-CCS) with ML models resulted in an average RMSE reduction of 21.7% for HBV and 24.9% for GR6J after decomposition, compared to simulations without decomposition. This enhanced capability contributes to better-informed decision-making in regions characterized by data scarcity, particularly crucial for water resource management. The practical implications of our findings extend to improved accuracy in discharge predictions, offering valuable insights for environmental policies and sustainable water resource utilization. As we navigate the complexities of hydrological modeling, this research lays a foundation for implementing innovative approaches that directly impact real-world water management scenarios.

CRediT authorship contribution statement

Awad M. Ali: Conceptualization, Data curation, Investigation, Methodology, Software, Visualization, Writing – original draft, Writing – review & editing. **Mohammed Abdallah:** Conceptualization, Data curation, Investigation, Methodology, Software, Visualization, Writing – original draft, Writing – review & editing. **Babak Mohammadi:** Investigation, Methodology, Writing – review & editing. **Hussam Eldin Elzain:** Investigation, Writing – review & editing.

Code and data availability

Data for this study was sourced from various repositories and agencies. Air temperature data above 2 meters was obtained from ERA5 (European Center for Medium-Range Weather Forecasts-ECMWF), accessible for download via the Copernicus Climate Data Store (https://cds.climate.copernicus.eu/). Potential evapotranspiration (PET) data was retrieved from Global Land Evaporation Amsterdam Model-GLEAM 3.7a, which is accessible through the GLEAM website (https://www.gleam.eu/). Additionally, PERSIANN family products were obtained from the Center for Hydrometeorology and Remote Sensing (CHRS) at the University of California, Irvine (https://chrsdata.eng.uci.edu/). However, rain gauge data, crucial for this study, is not publicly available and can be requested from the Ethiopian National Meteorological Agency website (http://www.ethiomet.gov.et/).

The models and analysis techniques employed in this study were implemented using various programming languages and packages. The GR6J model was executed in R Programming Language using the `airGR` package (https://hydrogr.github.io/airGR/), while the Random Forest Regression (RFR) model utilized the `randomForest` package in R (https://cran.r-project.org/package=randomForest/). Boosted Regression Forest (BRF) modeling was performed using the `grf` package in R (https://cran.r-project.org/package=grf/), and Variational Mode Decomposition was applied using the `VMDecomp` package in R (https://cran.r-project.org/package=VMDecomp/). Lastly, the Catboost Regression (CBR) model was developed in Python using the `catboost` package (https://pypi.org/project/catboost/). This comprehensive approach ensured a robust analysis framework for the study.

Declaration of competing interest

The authors declare that they have no known competing financial interests or personal relationships that could have appeared to influence the work reported in this paper.

Appendix A. Supplementary data

Supplementary material related to this article can be found online at https://doi.org/10.1016/j.ejrh.2025.102337.

Data availability

The accessibility to the used datasets and libraries are detailed in section “Code and data availability”.

References

Abdallah, M., Mohammadi, B., Nasiri, H., Katipoğlu, O.M., Abdalla, M.A.A., Ebadzadeh, M.M., 2023. Daily global solar radiation time series prediction using variational mode decomposition combined with multi-functional recurrent fuzzy neural network and quantile regression forests algorithm. Energy Rep. 10, 4198–4217. http://dx.doi.org/10.1016/j.egyr.2023.10.070, URL: https://www.sciencedirect.com/science/article/pii/S2352484723015068?via%3Dihub.

Ahmadi, F., Tohidi, M., Sadrianzade, M., 2023. Streamflow prediction using a hybrid methodology based on variational mode decomposition (VMD) and machine learning approaches. Appl. Water Sci. 13 (6), 135. http://dx.doi.org/10.1007/s13201-023-01943-0, URL: https://link.springer.com/content/pdf/10.1007/s13201-023-01943-0.pdf.

Alfieri, L., Pappenberger, F., Wetterhall, F., Haiden, T., Richardson, D., Salamon, P., 2014. Evaluation of ensemble streamflow predictions in Europe. J. Hydrol. 517, 913–922. http://dx.doi.org/10.1016/j.jhydrol.2014.06.035, URL: https://www.sciencedirect.com/science/article/pii/S0022169414004958?via%3Dihub.

Alghafli, K., Ali, A.M., Shi, X., Sloan, W., Obeid, A.A.A., Shamsudduha, M., 2023. Evaluation of runoff estimation from GRACE coupled with different meteorological gridded products over the Upper Blue Nile Basin. J. Hydrol. Reg. Stud. 50, 101545. http://dx.doi.org/10.1016/j.ejrh.2023.101545, URL: https://www.sciencedirect.com/science/article/pii/S221458182300232X.

Ali, A.M., Melsen, L.A., Teuling, A.J., 2023. Inferring reservoir filling strategies under limited-data-availability conditions using hydrological modeling and Earth observations: the case of the Grand Ethiopian Renaissance Dam (GERD). Hydrol. Earth Syst. Sci. 27 (21), 4057–4086. http://dx.doi.org/10.5194/hess-27-4057-2023, URL: https://hess.copernicus.org/articles/27/4057/2023/hess-27-4057-2023.pdf.

Ali, M., Prasad, R., Xiang, Y., Khan, M., Ahsan Farooque, A., Zong, T., Yaseen, Z.M., 2021. Variational mode decomposition based random forest model for solar radiation forecasting: New emerging machine learning technology. Energy Rep. 7, 6700–6717. http://dx.doi.org/10.1016/j.egyr.2021.09.113, URL: https://www.sciencedirect.com/science/article/pii/S2352484721009203.

Allam, M.M., 2017. Optimal land and water allocation to agriculture and hydropower in the Upper Blue Nile basin. URL: http://hdl.handle.net/1721.1/113470.

Alriah, M.A.A., Bi, S., Nkunzimana, A., Elameen, A.M., Sarfo, I., Ayugi, B., 2022. Multiple gridded-based precipitation products’ performance in Sudan’s different topographical features and the influence of the Atlantic Multidecadal Oscillation on rainfall variability in recent decades. Int. J. Climatol. 42 (16), 9539–9566. http://dx.doi.org/10.1002/joc.7845.

Andriambeloson, J.A., Paris, A., Calmant, S., Rakotondraompiana, S., 2020. Re-initiating depth-discharge monitoring in small-sized ungauged watersheds by combining remote sensing and hydrological modelling: a case study in Madagascar. Hydrol. Sci. J. 65 (16), 2709–2728. http://dx.doi.org/10.1080/02626667.2020.1833013.

Ashouri, H., Hsu, K.-L., Sorooshian, S., Braithwaite, D.K., Knapp, K.R., Cecil, L.D., Nelson, B.R., Prat, O.P., 2015. PERSIANN-CDR: Daily precipitation climate data record from multisatellite observations for hydrological and climate studies. Bull. Am. Meteorol. Soc. 96 (1), 69–83. http://dx.doi.org/10.1175/BAMS-D-13-00068.1, URL: https://journals.ametsoc.org/downloadpdf/view/journals/bams/96/1/bams-d-13-00068.1.pdf.

Asmamaw, D.K., 2015. A critical review of integrated river basin management in the upper Blue Nile river basin: the case of Ethiopia. Int. J. River Basin Manag. 13 (4), 429–442. http://dx.doi.org/10.1080/15715124.2015.1013037.

Bâ, K., Balcázar, L., Diaz, V., Ortiz, F., Gómez-Albores, M., Díaz-Delgado, C., 2018. Hydrological evaluation of PERSIANN-CDR rainfall over upper Senegal river and Bani river basins. Remote. Sens. 10 (12), 1884. http://dx.doi.org/10.3390/rs10121884.

Bárdossy, A., Anwar, F., 2023. Why do our rainfall–runoff models keep underestimating the peak flows? Hydrol. Earth Syst. Sci. 27 (10), 1987–2000. http://dx.doi.org/10.5194/hess-27-1987-2023, URL: https://hess.copernicus.org/articles/27/1987/2023/hess-27-1987-2023.pdf.

Behrangi, A., Khakbaz, B., Jaw, T.C., AghaKouchak, A., Hsu, K., Sorooshian, S., 2011. Hydrologic evaluation of satellite precipitation products over a mid-size basin. J. Hydrol. 397 (3–4), 225–237. http://dx.doi.org/10.1016/j.jhydrol.2010.11.043.

Bergström, S., 1995. The HBV model. Comput. Model. Watershed Hydrol. 443–476, URL: https://www.cabdirect.org/cabdirect/abstract/19961904773.
Bitew, M.M., Gebremichael, M., 2011. Assessment of satellite rainfall products for streamflow simulation in medium watersheds of the Ethiopian highlands. Hydrol. Earth Syst. Sci. 15 (4), 1147–1155. http://dx.doi.org/10.5194/hess-15-1147-2011, URL: https://hess.copernicus.org/articles/15/1147/2011/.
Bitew, M.M., Gebremichael, M., Ghebremichael, L.T., Bayissa, Y.A., 2012. Evaluation of high-resolution satellite rainfall products through streamflow simulation in a hydrological modeling of a small mountainous watershed in Ethiopia. J. Hydrometeorol. 13 (1), 338–350. http://dx.doi.org/10.1175/2011JHM1292.1, URL: https://journals.ametsoc.org/view/journals/hydr/13/1/2011jhm1292_1.xml.
Breiman, L., 2001. Random forests. Mach. Learn. 45 (1), 5–32. http://dx.doi.org/10.1023/A:1010933404324.
Bueechi, E., Fischer, M., Crocetti, L., Trnka, M., Grlj, A., Zappa, L., Dorigo, W., 2023. Crop yield anomaly forecasting in the pannonian basin using gradient boosting and its performance in years of severe drought. Agricult. Forest. Meterol. 340, 109596. http://dx.doi.org/10.1016/j.agrformet.2023.109596, URL: https://www.sciencedirect.com/science/article/pii/S0168192323002873.
Camici, S., Ciabatta, L., Massari, C., Brocca, L., 2018. How reliable are satellite precipitation estimates for driving hydrological models: A verification study over the Mediterranean area. J. Hydrol. 563, 950–961. http://dx.doi.org/10.1016/j.jhydrol.2018.06.067, URL: https://www.sciencedirect.com/science/article/pii/S002216941830489X.
Chen, S., Yang, Y., Peng, Z., Dong, X., Zhang, W., Meng, G., 2019. Adaptive chirp mode pursuit: Algorithm and applications. Mech. Syst. Signal Process. 116, 566–584. http://dx.doi.org/10.1016/j.ymssp.2018.06.052.
Conway, D., 2000. The climate and hydrology of the Upper Blue Nile River. Geogr. J. 166 (1), 49–62. http://dx.doi.org/10.1111/j.1475-4959.2000.tb00006.x.
Crochemore, L., Ramos, M.-H., Pechlivanidis, I.G., 2020. Can continental models convey useful seasonal hydrologic information at the catchment scale? Water Resour. Res. 56 (2), e2019WR025700, https://doi.org/10.1029/2019WR025700.
Dibike, Y.B., Solomatine, D.P., 2001. River flow forecasting using artificial neural networks. Phys. Chem. Earth Part B: Hydrol. Ocean. Atmos. 26 (1), 1–7. http://dx.doi.org/10.1016/S1464-1909(01)85005-X.
Digna, R.F., Mohamed, Y.A., Van Der Zaag, P., Uhlenbrook, S., Corzo, G.A., 2017. Nile River Basin modelling for water resources management–a literature review. Int. J. River Basin Manag. 15 (1), 39–52. http://dx.doi.org/10.1080/15715124.2016.1228656.
Dile, Y.T., Tekleab, S., Ayana, E.K., Gebrehiwot, S.G., Worqlul, A.W., Bayabil, H.K., Yimam, Y.T., Tilahun, S.A., Daggupati, P., Karlberg, L., 2018. Advances in water resources research in the Upper Blue Nile basin and the way forward: A review. J. Hydrol. 560, 407–423. http://dx.doi.org/10.1016/j.jhydrol.2018.03.042, URL: https://www.sciencedirect.com/science/article/pii/S0022169418302087?via%3Dihub.
Douna, V., Barraza, V., Grings, F., Huete, A., Restrepo-Coupe, N., Beringer, J., 2021. Towards a remote sensing data based evapotranspiration estimation in Northern Australia using a simple random forest approach. J. Arid. Environ. 191, 104513. http://dx.doi.org/10.1016/j.jaridenv.2021.104513, URL: https://www.sciencedirect.com/science/article/pii/S0140196321000793.
Dragomiretskiy, K., Zosso, D., 2013. Variational mode decomposition. IEEE Trans. Signal Process. 62 (3), 531–544. http://dx.doi.org/10.1109/TSP.2013.2288675, URL: https://ieeexplore.ieee.org/document/6655981/.
Eini, M.R., Rahmati, A., Piniewski, M.a., 2022. Hydrological application and accuracy evaluation of PERSIANN satellite-based precipitation estimates over a humid continental climate catchment. J. Hydrol. Reg. Stud. 41, 101109. http://dx.doi.org/10.1016/j.ejrh.2022.101109, URL: https://www.sciencedirect.com/science/article/pii/S2214581822001227?via%3Dihub.
Ekmekcioğlu, Ö., 2023. Drought forecasting using integrated variational mode decomposition and extreme gradient boosting. Water 15 (19), 3413. http://dx.doi.org/10.3390/w15193413, URL: http://dx.doi.org/10.3390/w15193413.
Elzain, H.E., Abdalla, O., A. Ahmed, H., Kacimov, A., Al-Maktoumi, A., Al-Higgi, K., Abdallah, M., Yassin, M.A., Senapathi, V., 2024. An innovative approach for predicting groundwater TDS using optimized ensemble machine learning algorithms at two levels of modeling strategy. J. Environ. Manag. 351, 119896. http://dx.doi.org/10.1016/j.jenvman.2023.119896, URL: https://www.sciencedirect.com/science/article/pii/S0301479723026841.
Friedman, J.H., 2001. Greedy function approximation: A gradient boosting machine. Ann. Statist. 29 (5), 1189–1232, URL: http://www.jstor.org/stable/2699986.
Gan, M., Pan, H., Chen, Y., Pan, S., 2021. Application of the variational mode decomposition (VMD) method to river tides. Estuar. Coast. Shelf Sci. 261, 107570. http://dx.doi.org/10.1016/j.ecss.2021.107570, URL: https://www.sciencedirect.com/science/article/pii/S0272771421004200.
Gebere, S., Alamirew, T., Merkel, B., Melesse, A., 2015. Performance of high resolution satellite rainfall products over data scarce parts of eastern Ethiopia. Remote. Sens. 7 (9), 11639–11663. http://dx.doi.org/10.3390/rs70911639, URL: http://dx.doi.org/10.3390/rs70911639.
Gebregiorgis, A.S., Hossain, F., 2012. Understanding the dependence of satellite rainfall uncertainty on topography and climate for hydrologic model simulation. IEEE Trans. Geosci. Remote Sens. 51 (1), 704–718. http://dx.doi.org/10.1109/tgrs.2012.2196282, URL: https://ieeexplore.ieee.org/document/6203572/.
Gebremicael, T.G., Deitch, M.J., Gancel, H.N., Croteau, A.C., Haile, G.G., Beyene, A.N., Kumar, L., 2022. Satellite-based rainfall estimates evaluation using a parsimonious hydrological model in the complex climate and topography of the Nile River Catchments. Atmos. Res. 266, 105939. http://dx.doi.org/10.1016/j.atmosres.2021.105939.
Giri, S., Kang, Y., MacDonald, K., Tippett, M., Qiu, Z., Lathrop, R.G., Obropta, C.C., 2023. Revealing the sources of arsenic in private well water using Random Forest Classification and Regression. Sci. Total Environ. 857, 159360. http://dx.doi.org/10.1016/j.scitotenv.2022.159360, URL: https://www.sciencedirect.com/science/article/pii/S0048969722064592.
Govindaraju, R.S., 2000. Artificial neural networks in hydrology. I: Preliminary concepts. J. Hydrol. Eng. 5 (2), 115–123. http://dx.doi.org/10.1061/(ASCE)1084-0699(2000)5:2(115), URL: https://www.ars.usda.gov/research/publications/publication/?seqNo115=119079.
Guermazi, E., Milano, M., Reynard, E., 2019. Performance evaluation of satellite-based rainfall products on hydrological modeling for a transboundary catchment in northwest Africa. Theor. Appl. Climatol. 138 (3), 1695–1713. http://dx.doi.org/10.1007/s00704-019-02928-3, URL: https://link.springer.com/article/10.1007/s00704-019-02928-3.
Gupta, H.V., Kling, H., Yilmaz, K.K., Martinez, G.F., 2009. Decomposition of the mean squared error and NSE performance criteria: Implications for improving hydrological modelling. J. Hydrol. 377 (1–2), 80–91. http://dx.doi.org/10.1016/j.jhydrol.2009.08.003, URL: http://dx.doi.org/10.1016/j.jhydrol.2009.08.003.
Harrison, J.W., Lucius, M.A., Farrell, J.L., Eichler, L.W., Relyea, R.A., 2021. Prediction of stream nitrogen and phosphorus concentrations from high-frequency sensors using random forests regression. Sci. Total Environ. 763, 143005. http://dx.doi.org/10.1016/j.scitotenv.2020.143005, URL: https://www.sciencedirect.com/science/article/pii/S0048969720365359.
He, X., Luo, J., Zuo, G., Xie, J., 2019. Daily runoff forecasting using a hybrid model based on variational mode decomposition and deep neural networks. Water Resour. Manag. 33, 1571–1590. http://dx.doi.org/10.1007/s11269-019-2183-x, URL: https://link.springer.com/article/10.1007/s11269-019-2183-x.
Hersbach, H., Bell, W., Berrisford, P., Horányi, A., J., M.-S., Nicolas, J., Radu, R., Schepers, D., Simmons, A., Soci, C., Dee, D., 2019. Global reanalysis: goodbye ERA-Interim, hello ERA5. ECMWF, http://dx.doi.org/10.21957/VF291HEHD7, URL: https://www.ecmwf.int/node/19027.
Hong, Y., Hsu, K.-L., Sorooshian, S., Gao, X., 2004. Precipitation estimation from remotely sensed imagery using an artificial neural network cloud classification system. J. Appl. Meteorol. 43 (12), 1834–1853. http://dx.doi.org/10.1175/JAM2173.1, URL: https://journals.ametsoc.org/downloadpdf/view/journals/apme/43/12/jam2173.1.pdf.
Hsu, K.-l., Gao, X., Sorooshian, S., Gupta, H.V., 1997. Precipitation estimation from remotely sensed information using artificial neural networks. J. Appl. Meteorol. Clim. 36 (9), 1176–1190. http://dx.doi.org/10.1175/1520-0450(1997)036<1176:PEFRSI>2.0.CO;2.
Hu, H., Zhang, J., Li, T., 2021. A novel hybrid decompose-ensemble strategy with a VMD-BPNN approach for daily streamflow estimating. Water Resour. Manag. 35 (15), 5119–5138. http://dx.doi.org/10.1007/s11269-021-02990-5, URL: https://link.springer.com/article/10.1007/s11269-021-02990-5.
Huang, G., Wu, L., Ma, X., Zhang, W., Fan, J., Yu, X., Zeng, W., Zhou, H., 2019. Evaluation of CatBoost method for prediction of reference evapotranspiration in humid regions. J. Hydrol. 574, 1029–1041. http://dx.doi.org/10.1016/j.jhydrol.2019.04.085, URL: https://www.sciencedirect.com/science/article/pii/S0022169419304251.

Hussien, D.M.A.E.-S., 2014. Improvement of precipitation estimation techniques over the Nile basin. URL: https://www.researchgate.net/profile/Doaa-Amin-2/publication/321213585_Improvement_of_Precipitation_Estimation_Techniques_over_the_Nile_Basin/links/5a1555c8458515005213358d/Improvement-of-Precipitation-Estimation-Techniques-over-the-Nile-Basin.pdf.

Jain Figueroa, A., 2012. Using a water balance model to analyze the implications of potential irrigation development in the Upper Blue Nile Basin. URL: http://hdl.handle.net/1721.1/72894.

Jiang, S., Wei, L., Ren, L., Xu, C.-Y., Zhong, F., Wang, M., Zhang, L., Yuan, F., Liu, Y., 2021. Utility of integrated IMERG precipitation and GLEAM potential evapotranspiration products for drought monitoring over mainland China. Atmos. Res. 247, 105141. http://dx.doi.org/10.1016/j.atmosres.2020.105141.

Kang, Y., Chen, P., Cheng, X., Zhang, S., Song, S., 2022. Novel hybrid machine learning framework with decomposition–transformation and identification of key modes for estimating reference evapotranspiration. Agricult. Water. Manag. 273, 107882. http://dx.doi.org/10.1016/j.agwat.2022.107882, URL: https://www.sciencedirect.com/science/article/pii/S0378377422004292.

Katipoğlu, O.M., Sarı göl, M., 2023. Application of boosted tree algorithm with new data preprocessing techniques in the forecasting one day ahead streamflow values in the Tigris basin, Türkiye. J. Hydro-Environ. Res. 50, 13–25. http://dx.doi.org/10.1016/j.jher.2023.07.004, URL: https://www.sciencedirect.com/science/article/pii/S1570644323000278.

Khan, S.I., Hong, Y., Wang, J., Yilmaz, K.K., Gourley, J.J., Adler, R.F., Brakenridge, G.R., Policelli, F., Habib, S., Irwin, D., 2010. Satellite remote sensing and hydrologic modeling for flood inundation mapping in Lake Victoria basin: Implications for hydrologic prediction in ungauged basins. IEEE Trans. Geosci. Remote Sens. 49 (1), 85–95. http://dx.doi.org/10.1109/TGRS.2010.2057513, URL: https://ieeexplore.ieee.org/document/5559412/.

Khoshchehreh, M., Ghomeshi, M., Shahbazi, A., 2020. Hydrological evaluation of global gridded precipitation datasets in a heterogeneous and data-scarce basin in Iran. J. Earth Syst. Sci. 129, 1–15. http://dx.doi.org/10.1007/s12040-020-01462-5, URL: https://link.springer.com/article/10.1007/s12040-020-01462-5.

Kim, U., Kaluarachchi, J.J., 2009. Climate change impacts on water resources in the upper blue Nile River Basin, Ethiopia 1. JAWRA J. Am. Water Resour. Assoc. 45 (6), 1361–1378. http://dx.doi.org/10.1111/j.1752-1688.2009.00369.x.

Kling, H., Fuchs, M., Paulin, M., 2012. Runoff conditions in the upper Danube basin under an ensemble of climate change scenarios. J. Hydrol. 424–425, 264–277. http://dx.doi.org/10.1016/j.jhydrol.2012.01.011, URL: http://dx.doi.org/10.1016/j.jhydrol.2012.01.011.

Krause, P., Boyle, D.P., Bäse, F., 2005. Comparison of different efficiency criteria for hydrological model assessment. Adv. Geosci. 5, 89–97. http://dx.doi.org/10.5194/adgeo-5-89-2005, URL: https://adgeo.copernicus.org/articles/5/89/2005/adgeo-5-89-2005.pdf.

Kumar, V., Kedam, N., Sharma, K.V., Mehta, D.J., Caloiero, T., 2023. Advanced machine learning techniques to improve hydrological prediction: a comparative analysis of streamflow prediction models. Water 15 (14), 2572. http://dx.doi.org/10.3390/w15142572, URL: https://mdpi-res.com/d_attachment/water/water-15-02572/article_deploy/water-15-02572-v2.pdf?version=1689306341.

Kumar, R.P., Sanjeeva, P., Lazarus, S.F., Dasari, V.K., 2019. An insight on machine learning algorithms and its applications. Int. J. Innov. Technol. Explor. Eng. 8 (11S2), 432–436. http://dx.doi.org/10.35940/ijitee.k1069.09811s219.

Kunnath-Poovakka, A., Eldho, T.I., 2023. Bias correction of satellite precipitation products for hydrologic modeling in Western Ghats Region, India. J. Hydrol. Eng. 28 (4), 04023010. http://dx.doi.org/10.1061/JHYEFF.HEENG-5699.

Lange, H., Sippel, S., 2020. Machine learning applications in hydrology. In: Levia, D.F., Carlyle-Moses, D.E., Iida, S., Michalzik, B., Nanko, K., Tischer, A. (Eds.), Forest-Water Interactions. Springer International Publishing, Cham, pp. 233–257. http://dx.doi.org/10.1007/978-3-030-26086-6_10.

Lary, D.J., Alavi, A.H., Gandomi, A.H., Walker, A.L., 2016. Machine learning in geosciences and remote sensing. Geosci. Front. 7 (1), 3–10. http://dx.doi.org/10.1016/J.GSF.2015.07.003, URL: https://www.sciencedirect.com/science/article/pii/S1674987115000821?via%3Dihub.

Lauri, H., Räsänen, T.A., Kummu, M., 2014. Using reanalysis and remotely sensed temperature and precipitation data for hydrological modeling in monsoon climate: Mekong river case study. J. Hydrometeorol. 15 (4), 1532–1545. http://dx.doi.org/10.1175/JHM-D-13-084.1, URL: https://journals.ametsoc.org/downloadpdf/view/journals/hydr/15/4/jhm-d-13-084_1.pdf.

Le, M.-H., Lakshmi, V., Bolten, J., Du Bui, D., 2020. Adequacy of satellite-derived precipitation estimate for hydrological modeling in Vietnam basins. J. Hydrol. 586, 124820. http://dx.doi.org/10.1016/j.jhydrol.2020.124820.

Li, X., Zhang, L., Zeng, S., Tang, Z., Liu, L., Zhang, Q., Tang, Z., Hua, X., 2022. Predicting monthly runoff of the upper Yangtze river based on multiple machine learning models. Sustainability 14 (18), 11149. http://dx.doi.org/10.3390/su141811149, URL: https://mdpi-res.com/d_attachment/sustainability/sustainability-14-11149/article_deploy/sustainability-14-11149-v2.pdf?version=1662532245.

Liu, X., Zhang, X., Kong, X., Shen, Y.-J., 2022. Random forest model has the potential for runoff simulation and attribution. Water 14 (13), 2053. http://dx.doi.org/10.3390/w14132053, URL: https://mdpi-res.com/d_attachment/water/water-14-02053/article_deploy/water-14-02053-v2.pdf?version=1656402933.

Ma, Y., Yang, Y., Han, Z., Tang, G., Maguire, L., Chu, Z., Hong, Y., 2018. Comprehensive evaluation of ensemble multi-satellite precipitation dataset using the dynamic Bayesian model averaging scheme over the tibetan plateau. J. Hydrol. 556, 634–644. http://dx.doi.org/10.1016/j.jhydrol.2017.11.050, URL: https://www.sciencedirect.com/science/article/pii/S0022169417308156.

Maswood, M., Hossain, F., 2016. Advancing river modelling in ungauged basins using satellite remote sensing: the case of the Ganges–Brahmaputra–Meghna basin. Int. J. River Basin Manag. 14 (1), 103–117. http://dx.doi.org/10.1080/15715124.2015.1089250.

McColl, K.A., Vogelzang, J., Konings, A.G., Entekhabi, D., Piles, M., Stoffelen, A., 2014. Extended triple collocation: Estimating errors and correlation coefficients with respect to an unknown target. Geophys. Res. Lett. 41 (17), 6229–6236. http://dx.doi.org/10.1002/2014gl061322, URL: http://dx.doi.org/10.1002/2014GL061322.

McNamara, I., Baez-Villanueva, O.M., Zomorodian, A., Ayyad, S., Zambrano-Bigiarini, M., Zaroug, M., Mersha, A., Nauditt, A., Mbuliro, M., Wamala, S., 2021. How well do gridded precipitation and actual evapotranspiration products represent the key water balance components in the Nile Basin? J. Hydrol. Reg. Stud. 37, 100884. http://dx.doi.org/10.1016/j.ejrh.2021.100884, URL: https://www.sciencedirect.com/science/article/pii/S2214581821001130?via%3Dihub.

Mengistu, D., Bewket, W., Dosio, A., Panitz, H.-J., 2021. Climate change impacts on water resources in the upper blue Nile (Abay) River Basin, Ethiopia. J. Hydrol. 592, 125614. http://dx.doi.org/10.1016/j.jhydrol.2020.125614.

Michel, C., 1987. Hydrologie appliquée aux petits bassins ruraux. Centre national du machinisme agricole, du génie rural, des eaux et des forêts, URL: https://side.developpement-durable.gouv.fr/Default/doc/SYRACUSE/162685/hydrologie-appliquee-aux-petits-bassins-ruraux.

Miralles, D.G., Holmes, T.R.H., De Jeu, R.A.M., Gash, J.H., Meesters, A., Dolman, A.J., 2011. Global land-surface evaporation estimated from satellite-based observations. Hydrol. Earth Syst. Sci. 15 (2), 453–469. http://dx.doi.org/10.5194/hess-15-453-2011, URL: https://hess.copernicus.org/articles/15/453/2011/hess-15-453-2011.pdf.

Mohammadi, B., Vazifehkhah, S., Duan, Z., 2024. A conceptual metaheuristic-based framework for improving runoff time series simulation in glacierized catchments. Eng. Appl. Artif. Intell. 127, 107302. http://dx.doi.org/10.1016/j.engappai.2023.107302, URL: https://www.sciencedirect.com/science/article/pii/S0952197623014860?via%3Dihub.

Moriasi, D.N., Arnold, J.G., Liew, M.W.V., Bingner, R.L., Harmel, R.D., Veith, T.L., 2007. Model evaluation guidelines for systematic quantification of accuracy in watershed simulations. Trans. the ASABE 50 (3), 885–900. http://dx.doi.org/10.13031/2013.23153, URL: http://dx.doi.org/10.13031/2013.23153.

Mosaffa, H., Sadeghi, M., Mallakpour, I., Jahromi, M.N., Pourghasemi, H.R., 2022. Application of machine learning algorithms in hydrology. In: Computers in Earth and Environmental Sciences. Elsevier, pp. 585–591. http://dx.doi.org/10.1016/B978-0-323-89861-4.00027-0.

Musie, M., Sen, S., Srivastava, P., 2019. Comparison and evaluation of gridded precipitation datasets for streamflow simulation in data scarce watersheds of ethiopia. J. Hydrol. 579, 124168. http://dx.doi.org/10.1016/j.jhydrol.2019.124168, URL: https://www.sciencedirect.com/science/article/pii/S0022169419309035.

Nash, J., Sutcliffe, J., 1970. River flow forecasting through conceptual models part i — A discussion of principles. J. Hydrol. 10 (3), 282–290. http://dx.doi.org/10.1016/0022-1694(70)90255-6, URL: http://dx.doi.org/10.1016/0022-1694(70)90255-6.

Nasr, H., Neef, A., 2016. Ethiopia's challenge to Egyptian hegemony in the Nile River Basin: the case of the grand Ethiopian Renaissance Dam. Geopolitics 21 (4), 969–989. http://dx.doi.org/10.1080/14650045.2016.1209740.

Nawaz, M., Iqbal, M.F., Mahmood, I., 2021. Validation of CHIRPS satellite-based precipitation dataset over Pakistan. Atmos. Res. 248, 105289. http://dx.doi.org/10.1016/j.atmosres.2020.105289, URL: https://www.sciencedirect.com/science/article/pii/S0169809520312266.

Nguyen, N.T., Du, T.L.T., Park, H., Chang, C.-H., Choi, S., Chae, H., Nelson, E.J., Hossain, F., Kim, D., Lee, H., 2023. Estimating the impacts of ungauged reservoirs using publicly available streamflow simulations and satellite remote sensing. Remote. Sens. 15 (18), 4563. http://dx.doi.org/10.3390/rs15184563, URL: http://dx.doi.org/10.3390/rs15184563.

Nguyen, P., Ombadi, M., Sorooshian, S., Hsu, K., AghaKouchak, A., Braithwaite, D., Ashouri, H., Thorstensen, A.R., 2018. The PERSIANN family of global satellite precipitation data: A review and evaluation of products. Hydrol. Earth Syst. Sci. 22 (11), 5801–5816. http://dx.doi.org/10.5194/hess-22-5801-2018, URL: https://hess.copernicus.org/articles/22/5801/2018/hess-22-5801-2018.pdf.

Okkan, U., Ersoy, Z.B., Kumanlioglu, A.A., Fistikoglu, O., 2021. Embedding machine learning techniques into a conceptual model to improve monthly runoff simulation: A nested hybrid rainfall-runoff modeling. J. Hydrol. 598, 126433. http://dx.doi.org/10.1016/j.jhydrol.2021.126433.

Poncelet, C., Merz, R., Merz, B., Parajka, J., Oudin, L., Andréassian, V., Perrin, C., 2017. Process-based interpretation of conceptual hydrological model performance using a multinational catchment set. Water Resour. Res. 53 (8), 7247–7268. http://dx.doi.org/10.1002/2016WR019991.

Poortinga, A., Bastiaanssen, W., Simons, G., Saah, D., Senay, G., Fenn, M., Bean, B., Kadyszewski, J., 2017. A self-calibrating runoff and streamflow remote sensing model for ungauged basins using open-access earth observation data. Remote. Sens. 9 (1), 86. http://dx.doi.org/10.3390/rs9010086.

Prokhorenkova, L., Gusev, G., Vorobev, A., Dorogush, A.V., Gulin, A., 2018. CatBoost: unbiased boosting with categorical features. Adv. Neural Inf. Process. Syst. 31, URL: https://proceedings.neurips.cc/paper_files/paper/2018/file/14491b756b3a51daac41c24863285549-Paper.pdf.

Pushpalatha, R., Perrin, C., Le Moine, N., Mathevet, T., Andréassian, V., 2011. A downward structural sensitivity analysis of hydrological models to improve low-flow simulation. J. Hydrol. 411 (1–2), 66–76. http://dx.doi.org/10.1016/j.jhydrol.2011.09.034.

Rehman, N., Mandic, D.P., 2010. Multivariate empirical mode decomposition. Proc. R. Soc. A: Math. Phys. Eng. Sci. 466 (2117), 1291–1302. http://dx.doi.org/10.1098/rspa.2009.0502.

Roy, A., Kasiviswanathan, K.S., Patidar, S., Adeloye, A.J., Soundharajan, B.-S., Ojha, C.S.P., 2023. A novel physics-aware machine learning-based dynamic error correction model for improving streamflow forecast accuracy. Water Resour. Res. 59 (2), e2022WR033318, https://doi.org/10.1029/2022WR033318.

Sadeghi, M., Nguyen, P., Naeini, M.R., Hsu, K., Braithwaite, D., Sorooshian, S., 2021. PERSIANN-CCS-CDR, a 3-hourly 0.04 global precipitation climate data record for heavy precipitation studies. Sci. Data 8 (1), 157. http://dx.doi.org/10.1038/s41597-021-00940-9, URL: https://www.nature.com/articles/s41597-021-00940-9.pdf.

Salehi, H., Sadeghi, M., Golian, S., Nguyen, P., Murphy, C., Sorooshian, S., 2022. The application of PERSIANN family datasets for hydrological modeling. Remote. Sens. 14 (15), 3675. http://dx.doi.org/10.3390/rs14153675, URL: https://mdpi-res.com/d_attachment/remotesensing/remotesensing-14-03675/article_deploy/remotesensing-14-03675-v2.pdf?version=1659961310.

Samani, S., Vadiati, M., Delkash, M., Bonakdari, H., 2023. A hybrid wavelet–machine learning model for qanat water flow prediction. Acta Geophys. 71 (4), 1895–1913. http://dx.doi.org/10.1007/s11600-022-00964-8, URL: https://link.springer.com/article/10.1007/s11600-022-00964-8.

Satgé, F., Ruelland, D., Bonnet, M.P., Molina, J., Pillco, R., 2019. Consistency of satellite-based precipitation products in space and over time compared with gauge observations and snow- hydrological modelling in the lake titicaca region. Hydrol. Earth Syst. Sci. 23 (1), 595–619. http://dx.doi.org/10.5194/hess-23-595-2019, URL: https://hess.copernicus.org/articles/23/595/2019/hess-23-595-2019.pdf.

Seo, Y., Kim, S., Singh, V.P., 2018. Machine learning models coupled with variational mode decomposition: a new approach for modeling daily rainfall-runoff. Atmosphere 9 (7), 251. http://dx.doi.org/10.3390/atmos9070251, URL: https://mdpi-res.com/d_attachment/atmosphere/atmosphere-09-00251/article_deploy/atmosphere-09-00251.pdf?version=1530786662.

Sezen, C., Partal, T., 2022. New hybrid GR6j-wavelet-based genetic algorithm-artificial neural network (GR6j-WGANN) conceptual-data-driven model approaches for daily rainfall–runoff modelling. Neural Comput. Appl. 34 (20), 17231–17255. http://dx.doi.org/10.1007/s00521-022-07372-5, URL: https://link.springer.com/article/10.1007/s00521-022-07372-5.

Shayeghi, A., Azizian, A., Brocca, L., 2020. Reliability of reanalysis and remotely sensed precipitation products for hydrological simulation over the Sefidrood River Basin, Iran. Hydrol. Sci. J. 65 (2), 296–310. http://dx.doi.org/10.1080/02626667.2019.1691217.

Sibtain, M., Li, X., Bashir, H., Azam, M.I., 2021. A hybrid model for runoff prediction using variational mode decomposition and artificial neural network. Water Resour. 48, 701–712. http://dx.doi.org/10.1134/S0097807821050171, URL: https://link.springer.com/article/10.1134/S0097807821050171.

Sorooshian, S., Hsu, K.-L., Gao, X., Gupta, H.V., Imam, B., Braithwaite, D., 2000. Evaluation of PERSIANN system satellite-based estimates of tropical rainfall. Bull. Am. Meteorol. Soc. 81 (9), 2035–2046. http://dx.doi.org/10.1175/1520-0477(2000)081<2035:EOPSSE>2.3.CO;2.

Steinfeld, C.M.M., Kingsford, R.T., Webster, E.C., Sharma, A., 2015. A simulation tool for managing environmental flows in regulated rivers. Environ. Model. Softw. 73, 117–132. http://dx.doi.org/10.1016/j.envsoft.2015.08.006.

Stoffelen, A., 1998. Toward the true near-surface wind speed: Error modeling and calibration using triple collocation. J. Geophys. Res. Ocean. 103 (C4), 7755–7766. http://dx.doi.org/10.1029/97jc03180, URL: http://dx.doi.org/10.1029/97JC03180.

Tan, X.Z., Li, Y., Wu, X.X., Dai, C., Zhang, X.L., Cai, Y.P., 2024. Identification of the key driving factors of flash flood based on different feature selection techniques coupled with random forest method. J. Hydrol. Reg. Stud. 51, 101624. http://dx.doi.org/10.1016/j.ejrh.2023.101624, URL: https://www.sciencedirect.com/science/article/pii/S2214581823003117.

Taylor, K.E., 2001. Summarizing multiple aspects of model performance in a single diagram. J. Geophys. Res. Atmos. 106 (D7), 7183–7192. http://dx.doi.org/10.1029/2000JD900719.

Tekleab, S., Mohamed, Y., Uhlenbrook, S., 2013. Hydro-climatic trends in the Abay/upper Blue Nile basin, Ethiopia. Phys. Chem. Earth, Parts A/ B/ C 61, 32–42. http://dx.doi.org/10.1016/j.pce.2013.04.017.

Turhan, Y., 2021. The hydro-political dilemma in Africa water geopolitics: The case of the Nile river basin. Afr. Secur. Rev. 30 (1), 66–85. http://dx.doi.org/10.1080/10246029.2020.1844775.

Ur Rahman, K., Shang, S., Shahid, M., Wen, Y., 2020. Hydrological evaluation of merged satellite precipitation datasets for streamflow simulation using SWAT: A case study of Potohar Plateau, Pakistan. J. Hydrol. 587, 125040. http://dx.doi.org/10.1016/j.jhydrol.2020.125040, URL: https://www.sciencedirect.com/science/article/pii/S002216942030500X.

Wang, H., Kang, C., Tian, Z., Zhang, A., Cao, Y., 2023a. Vegetation periodic changes and relationships with climate in inner Mongolia based on the VMD method. Ecol. Indic. 146, 109764. http://dx.doi.org/10.1016/j.ecolind.2022.109764, URL: https://www.sciencedirect.com/science/article/pii/S1470160X22012377.

Wang, Q., Li, Z., Cai, J., Zhang, M., Liu, Z., Xu, Y., Li, R., 2023b. Spatially adaptive machine learning models for predicting water quality in Hong Kong. J. Hydrol. 622, 129649. http://dx.doi.org/10.1016/j.jhydrol.2023.129649, URL: https://www.sciencedirect.com/science/article/pii/S0022169423005917.

Wang, C., Si, J., Li, Z., Zhao, C., Jia, B., Celestin, S., He, X., Zhou, D., Qin, J., Zhu, X., 2022. Evaluation of three gridded potential evapotranspiration datasets for streamflow simulation in three inland river basins in the arid Hexi Corridor, Northwest China. J. Hydrol. Reg. Stud. 44, 101234. http://dx.doi.org/10.1016/j.ejrh.2022.101234, URL: https://www.sciencedirect.com/science/article/pii/S2214581822002476?via%3Dihub.

Wang, Q., Xia, J., She, D., Zhang, X., Liu, J., Zhang, Y., 2021. Assessment of four latest long-term satellite-based precipitation products in capturing the extreme precipitation and streamflow across a humid region of southern China. Atmos. Res. 257, 105554. http://dx.doi.org/10.1016/j.atmosres.2021.105554.

Wen, X., Feng, Q., Deo, R.C., Wu, M., Yin, Z., Yang, L., Singh, V.P., 2019. Two-phase extreme learning machines integrated with the complete ensemble empirical mode decomposition with adaptive noise algorithm for multi-scale runoff prediction problems. J. Hydrol. 570, 167–184. http://dx.doi.org/10.1016/j.jhydrol.2018.12.060, URL: https://www.sciencedirect.com/science/article/pii/S0022169419300381.

Wu, J., Wang, Z., Dong, J., Cui, X., Tao, S., Chen, X., 2023a. Robust runoff prediction with explainable artificial intelligence and meteorological variables from deep learning ensemble model. Water Resour. Res. 59 (9), e2023WR035676, https://doi.org/10.1029/2023WR035676.

Wu, J., Wang, Z., Hu, Y., Tao, S., Dong, J., 2023b. Runoff forecasting using convolutional neural networks and optimized bi-directional long short-term memory. Water Resour. Manag. 37 (2), 937–953. http://dx.doi.org/10.1007/s11269-022-03414-8, URL: http://dx.doi.org/10.1007/s11269-022-03414-8.

Xiao, S., Zou, L., Xia, J., Yang, Z., Yao, T., 2022. Bias correction framework for satellite precipitation products using a rain/no rain discriminative model. Sci. Total Environ. 818, 151679. http://dx.doi.org/10.1016/j.scitotenv.2021.151679, URL: https://www.sciencedirect.com/science/article/pii/S0048969721067553.

Xiong, J., Guo, S., Yin, J., 2021. Discharge estimation using integrated satellite data and hybrid model in the midstream Yangtze River. Remote. Sens. 13 (12), 2272. http://dx.doi.org/10.3390/rs13122272, URL: https://mdpi-res.com/d_attachment/remotesensing/remotesensing-13-02272/article_deploy/remotesensing-13-02272.pdf?version=1623319881.

Xu, X., Li, J., Tolson, B.A., 2014. Progress in integrating remote sensing data and hydrologic modeling. Prog. Phys. Geogr. 38 (4), 464–498. http://dx.doi.org/10.1177/0309133314536583.

Yaseen, Z.M., El-Shafie, A., Jaafar, O., Afan, H.A., Sayl, K.N., 2015. Artificial intelligence based models for stream-flow forecasting: 2000–2015. J. Hydrol. 530, 829–844. http://dx.doi.org/10.1016/j.jhydrol.2015.10.038.

Yu, Q., Jiang, L., Wang, Y., Liu, J., 2023. Enhancing streamflow simulation using hybridized machine learning models in a semi-arid basin of the Chinese loess Plateau. J. Hydrol. 617, 129115. http://dx.doi.org/10.1016/j.jhydrol.2023.129115.

Zhang, X., Wang, X., Li, H., Sun, S., Liu, F., 2023. Monthly runoff prediction based on a coupled VMD-SSA-BiLSTM model. Sci. Rep. 13 (1), 13149. http://dx.doi.org/10.1038/s41598-023-39606-4, URL: https://www.nature.com/articles/s41598-023-39606-4.pdf.

Zhu, Q., Xuan, W., Liu, L., Xu, Y.-P., 2016. Evaluation and hydrological application of precipitation estimates derived from PERSIANN-CDR, TRMM 3B42V7, and NCEP-CFSR over humid regions in China. Hydrol. Process. 30 (17), 3061–3083. http://dx.doi.org/10.1002/hyp.10846.

Zounemat-Kermani, M., Batelaan, O., Fadaee, M., Hinkelmann, R., 2021. Ensemble machine learning paradigms in hydrology: A review. J. Hydrol. 598, 126266. http://dx.doi.org/10.1016/j.jhydrol.2021.126266, URL: https://www.sciencedirect.com/science/article/pii/S0022169421003139.

Zuo, G., Luo, J., Wang, N., Lian, Y., He, X., 2020. Decomposition ensemble model based on variational mode decomposition and long short-term memory for streamflow forecasting. J. Hydrol. 585, 124776. http://dx.doi.org/10.1016/j.jhydrol.2020.124776.